X-701-69-173
TASK III

NASA 63592

TECHNIQUES FOR ACHIEVING MAGNETIC CLEANLINESS ON DEEP-SPACE MISSIONS

A REPORT COVERING TASK III EFFORT
UNDER THE STUDY

NASA EVALUATION WITH MODELS OF OPTIMIZED NUCLEAR SPACECRAFT (NEW MOONS)

Wm. S. West, J. Michael Holman, and Herbert W. Bilsky

APRIL 1969

GSFC
GODDARD SPACE FLIGHT CENTER
GREENBELT, MARYLAND

X-701-69-173
TASK III

TECHNIQUES FOR ACHIEVING MAGNETIC CLEANLINESS ON DEEP-SPACE MISSIONS

A Report Covering Task III Effort Under The Study

NASA Evaluation With Models Of Optimized Nuclear Spacecraft
(NEW MOONS)

Wm. S. West, Technical Officer
Goddard Space Flight Center
Greenbelt, Maryland

and

J. Michael L. Holman and Herbert W. Bilsky
RCA
Astro-Electronics Division
Defense Electronic Products
Princeton, New Jersey

April 1969

GODDARD SPACE FLIGHT CENTER
Greenbelt, Maryland 70771

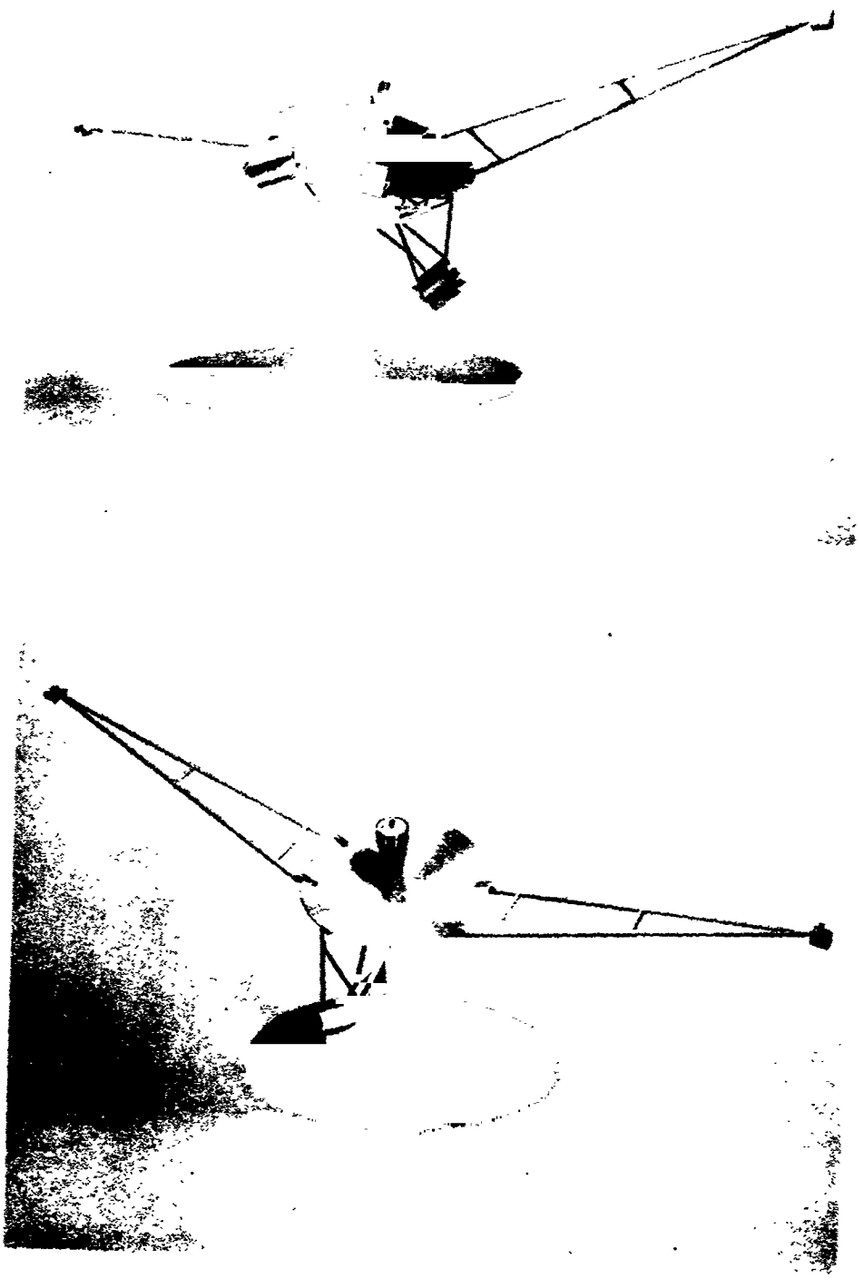

Frontispiece A–Two Views of a Model of the Galactic Jupiter Probe which served as the "Reference Design" for this Task

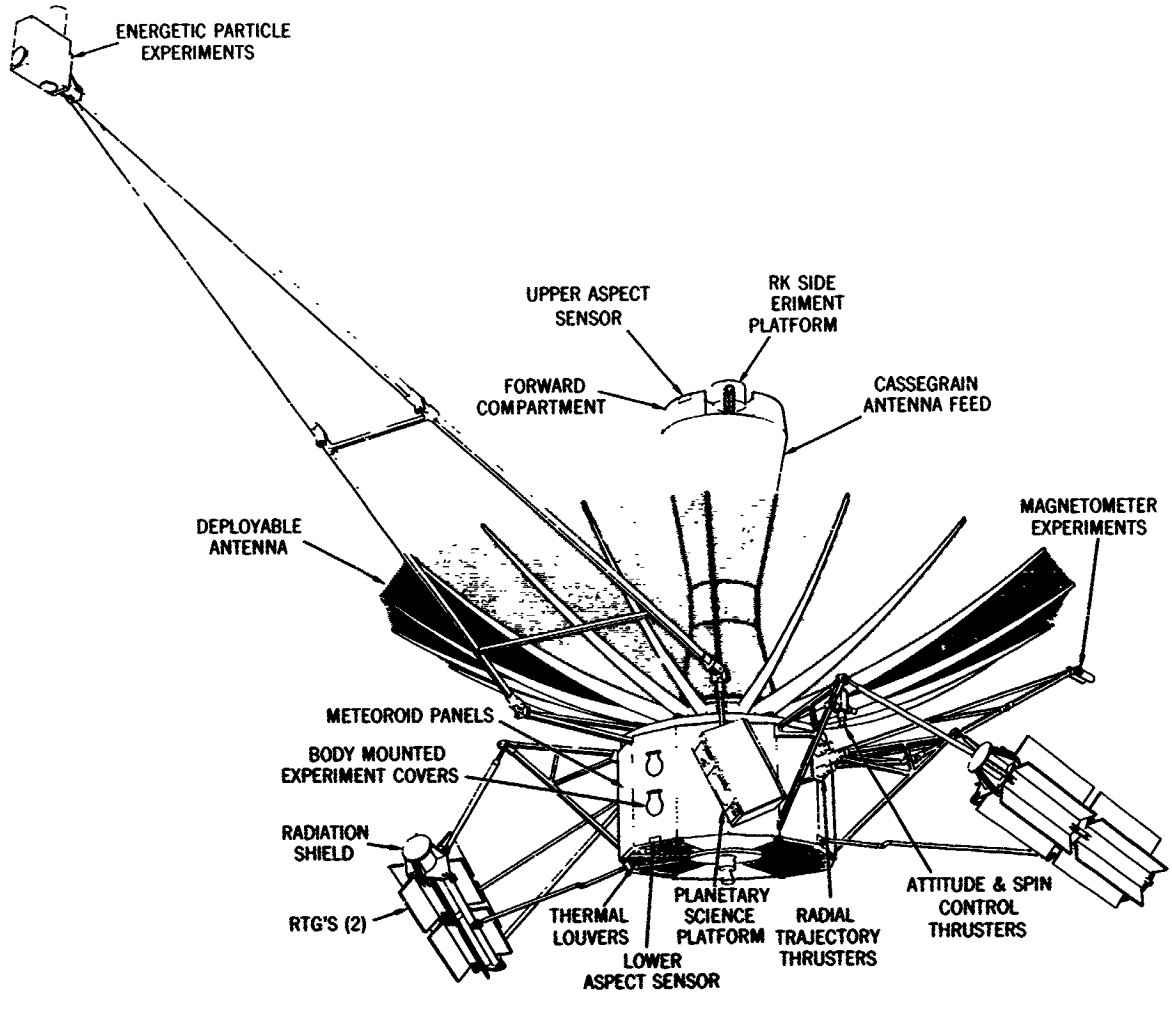

Frontispiece B–Outer Planets Explorer

TECHNIQUES FOR ACHIEVING MAGNETIC CLEANLINESS ON DEEP-SPACE MISSIONS

A Report Covering Task III Effort Under The Study

NASA Evaluation With Models Of Optimized Nuclear Spacecraft*
(NEW MOONS)

ABSTRACT

Unmanned spacecraft have been studied for missions to Jupiter and beyond that will obtain scientific data including measurements of magnetic fields in interplanetary space. This report describes engineering considerations associated with design, development and test of spacecraft and subsystems thereof that achieve sufficiently low levels of magnetic interference levels at the magnetometers to permit scientific measurement. Engineering methods and data are provided for selecting different background interference values; with 0.1 gamma being the value selected for illustration purposes in the study. Unique magnetic-considerations associated with nuclear power supplies are covered. Selected test data are presented.

*NASA Evaluation With Models Of Optimized Nuclear Spacecraft (NEW MOONS) Contract NAS 5-10441, performed by RCA Astro-Electronics Division, Defense Electronic Products, Princeton, New Jersey for NASA Goddard Space Flight Center, Greenbelt, Maryland.

LIST OF PERTINENT INFORMATION

1 gauss = 10^5 gamma = 10^{-4} Weber/m^2 (Tesla)

1 pole-cm = 10 amp-cm^2

Earth's magnetic field at the equator is 0.3 gauss

Jupiter's magnetic field at 3 R_J is of the order of 1.0 gauss

The field due to a dipole varies inversely as the distance cubed, $\frac{1}{r^3}$

The field due to a quadrupole varies inversely as the distance to the fourth power, $\frac{1}{r^4}$

The interplanetary magnetic field at 30 R_E from Earth in the direction of the Sun has a time averaged value of approximately 5 gamma (as measured by IMP).

The interplanetary magnetic field which is "frozen in" to the solar wind has a radial and tangential component whose vector sum describes a spiral.

The limits of the organized interplanetary magnetic field are thought to be somewhere between 10 AU and 100 AU.

ACKNOWLEDGMENT

Techniques for Achieving Magnetic Cleanliness on Deep-Space Missions

NEW MOONS Task III

PROGRAM:

In the course of conducting the studies of the NEW MOONS program valuable assistance has been provided by many people representing various organizations. It is considered appropriate to identify those whose contributions were most vital.

Fred Schulman, NASA Office of Advanced Research and Technology and Marcel Aucremanne, NASA Office of Space Science and Applications both realized the necessity for the NEW MOONS studies and provided technical guidance and financial support throughout the program.

Daniel G. Mazur, Assistant Director for Technology and Rudolph A. Stampfl, Deputy Assistant Director both of Goddard Space Flight Center aided in program initiation.

RCA Astro-Electronics Division, the prime contractor, recognized the importance of the NEW MOONS program and has given its support and cooperation toward realizing the objectives of the program. Herbert Bilsky served in the capacity of RCA project manager and technically contributed to the program as well as provided aid in preparation and review of this report.

REPORT PREPARATION:

J. Michael L. Holman of RCA AED prepared the original draft of the report and was the principal investigator. N. F. Campbell, SNAP-19 Program Manager, of ISOTOPES, Nuclear Systems Division of Teledyne Company, provided Appendix V, SNAP-19 Magnetic Flux Distribution. At Goddard, James H. Trainor provided information regarding scientific objectives and reviewed the final draft. Arthur W. Fihelly provided Appendix III, and D. W. Harris provided information in Appendix IV — both data based on SNAP-19 generator tests. Joseph Epstein, Emil W. Hymowitz and Joseph H. Conn reviewed, and commented upon, the complete report.

William S. West

William S. West, Technical Officer
Goddard Space Flight Center
Greenbelt, Maryland

PREFACE

BACKGROUND AND RELATED INFORMATION

Since the early 1960's, personnel of the Goddard Space Flight Center have been interested in deep-space missions to obtain information concerning the planets, Jupiter, Saturn, Uranus, Neptune and Pluto, as well as information concerning the interplanetary medium. Studies have been performed to establish the feasibility of such missions and various reports were written by Goddard personnel[1] and by others[2].

For almost as long as these missions have been considered, the engineers, scientists and managers at Goddard have realized the necessity for systems, independent of the Sun's energy, to supply the spacecraft electric power requirement. In general, Goddard studies have indicated that there is a weight advantage in using small nuclear power systems such as radioisotope fueled thermoelectric generators instead of presently available solar cells when missions go beyond 2.5 or 3 AU[3]. Further, there are technological and practical uncertainties in projecting use of solar arrays in a range starting beyond 3-5 AU[4] whereas the use of small nuclear power supplies is technically and practically feasible. However, the use of small nuclear systems, while feasible, nevertheless presents technical questions. An in-house Goddard study[5] identified pertinent technological areas requiring study prior to the use of these nuclear generators on spacecraft designed for scientific deep space missions.[6] These areas were divided into the following numbered tasks:

[1] A selected list of Goddard Space Flight Center deep-space reports is presented in Task I report X-701-69-170.

[2] A limited list of deep-space reports prepared by other centers and contractors is presented in X-701-69-170.

[3] See X-701-69-170 for references.

[4] Technical uncertainties involve practical design questions arising from the use of very large solar array areas, their survival through meteroid belts and their system performance when operating at the low temperature and low illumination levels anticipated.

[5] See NEW MOONS X-730-66-117 dated 1966.

[6] This study is referred to as NEW MOONS.

Task Number	Task Description — Title	Reference X Document
I	Analysis of Selected Deep-Space Missions	X-701-69-170
IIA	Subsystem Radiation Susceptibility Analysis of Deep-Space Missions	X-701-69-171
IIB	Spacecraft Charge Build-Up Analysis	X-701-69-172
III	Techniques for Achieving Magnetic Cleanliness	X-701-69-173
IV	Weight Minimization Analysis	X-701-69-174
V	Spacecraft Analysis and Design	X-701-69-175
VI	Spacecraft Test Documentation	X-701-69-176
VIIA	Planar RTG-Component Feasibility Study	X-701-69-177
VIIB	Planar RTG-Spacecraft Feasibility Study	X-701-69-178
VIII	RTG Interface Specification	X-701-69-179
	Summary Report of NEW MOONS	X-701-69-190

A contract[7] was established for further study of these areas. This study was entitled NASA Evaluation With Models Of Optimized Nuclear Spacecraft (NEW MOONS). During the execution of the NEW MOONS Technology Study, Goddard was assigned the task of conducting a Phase A study covering a Galactic Jupiter Probe[8]. These two study efforts, Galactic Jupiter Probe and NEW MOONS, were directed to provide the maximum practical benefit to each other. In general, the Galactic Jupiter Probe was considered as a "base line spacecraft and mission" or a "reference design" during the NEW MOONS Technology Study. On the other hand, the Galactic Jupiter Probe Study team made use of the technology and data as developed by the NEW MOONS Study in areas of missions analysis, shielding, aerospace nuclear safety, thermal and structural analysis and other related areas.

[7]NAS-5-10441 RCA Astro-Electronics Division, Princeton, N. J.

[8]See Advanced Nuclear Systems Study, GSFC X-716-67-323 dated July 1967; see Frontispiece A.

SPECIFIC RATIONALE FOR TASK III

The deep-space mission studies generally and particularly the studies covering both The Galactic Jupiter Probe and Outer Planet Explorers have as an important scientific objective, the acquisition of data concerning magnetic fields in interplanetary space. These magnetic field measurements are expected to extend to rather low levels (i.e., down to approximately 1 gamma or less). Spacecraft, and elements thereof, may have magnetic fields of their own which may mask the naturally occurring fields if special care is not taken. This Task, presents data based on prior spacecraft and RTG-hardware experience and postulated techniques for designing complete systems to meet stated scientific objectives. Particular attention is directed to the nuclear power supplies as they can represent a significant source of interference. Methods of improvement are indicated. Finally test procedures are suggested that might be relevant to program planners.

As the NEW MOONS contract was being concluded, the scope of Galactic Jupiter Probe project was broadened and adopted the name Outer Planets Explorer (OPE)[9]. The Outer Planet Explorer is considered for a generally more ambitious program than the original Galactic Jupiter Probe, in that the OPE is intended for a family of single and multiple planet missions.

The OPE, as presently visualized, encompasses spacecraft in the 1100-1400 pound class whereas the GJP "reference design-spacecraft" for the NEW MOONS Study was 500-600 pounds. This is a significant practical difference from a flight project viewpoint; however, the technology and techniques of NEW MOONS are generally applicable. Specific numeric values will be different when solutions are developed, but the techniques and rationale indicated in the NEW MOONS reports are applicable to the general problem of integrating and using small nuclear power systems on a scientific spacecraft designed for deep space missions.

APPLICABILITY TO OTHER PROGRAMS

The NEW MOONS technology and techniques reported may have applicability or some relevancy to additional space missions that may in the future use nuclear systems such as planetary landers and rovers as well as applications spacecraft.

[9]See Outer Planets Explorer (OPE), GSFC X-701-69-189, see Frontispiece B.

CONTENTS

CONTENTS (Continued)

CONTENTS (Continued)

APPENDIXES

LIST OF ILLUSTRATIONS

LIST OF ILLUSTRATIONS (Continued)

LIST OF TABLES

LIST OF TABLES (Continued)

TECHNIQUES FOR ACHIEVING MAGNETIC CLEANLINESS ON DEEP SPACE MISSIONS

A Report Covering Task III Effort Under The Study

NASA Evaluation With Models Of Optimized Nuclear Spacecraft (NEW MOONS)

SECTION I

INTRODUCTION AND SUMMARY

A. INTRODUCTION

Among the principal scientific objectives of the NEW MOONS or deep-space mission, along with radiation measurements of the space environment, is the mapping of the interplanetary magnetic field. The interplanetary medium is characterized by a weak magnetic field embedded in a radial plasma flux emitted from the surface of the Sun. The time-averaged value of the interplanetary magnetic field at 1 AU is 5 gamma and decreases inversely with distance from the Sun (Ref. 2).

Using this simplified model of the magnetic field, which does not take account of time variations in solar wind velocity or field magnitude, the average value of the interplanetary magnetic field is extrapolated to be approximately 1 gamma at 5 AU and 0.5 gamma at 10 AU. In order to measure fluctuations in a magnetic field of this level, background noise at the magnetometer due to residual magnetism and current loops in the spacecraft and the RTG's should be held to a combined total of no more than 0.1 gamma (Ref. 3).

Previous experience with SNAP generators in the IMP-1 and NIMBUS-B programs have shown that attempts to match an RTG developed without low magnetic field criteria with a scientific spacecraft intended for measurement of low fields can lead to technical incompatibility. In particular, tests on the SNAP-9A and SNAP-27 (Ref. 4) have shown that these generators are large sources of magnetic contamination. The magnetic interaction of the power subsystem and the scientific experiments in deep-space missions, therefore, requires careful consideration.

Task III has the following objectives and is specifically devoted to examining those parameters which affect the magnetic requirements of the spacecraft subsystems.

- Analyze the magnetic cleanliness constraints appropriate to the NEW MOONS missions,

- Study design techniques for minimizing magnetic fields associated with RTG' to meet these constraints, and

- Prepare a test program to demonstrate the effectiveness of the design techniques proposed.

The experience gained in producing magnetically clean spacecraft on both the IMP and the Pioneer programs has been applied to the Galactic Jupiter Probe (GJP) spacecraft (Ref. 5) which was chosen as the working model when establishing specification limits for this task. Various RTG configurations were investigated with emphasis on properties of materials, and consideration was given to circuit arrangements with respect to thermoelectric-element current loops.

To meet the objectives of this Task, the following steps have been taken:

- The magnitude of the magnetic fields to be measured was established.

- The tolerable magnetic background noise levels at the detector (s), consistent with the magnitude of the measurements to be made, were established.

- The magnetic fields produced by two different-type RTG's, planar and cylindrical, were evaluated.

- The source of magnetic field output in each type of the RTG's was identified.

- A means for minimizing the source of magnetic contamination from each of the two types of RTG's was determined.

- Appropriate RTG-sensor separation distances were established compatible with spacecraft weight minimization and dynamic constraints.

- The combined contribution to the background noise by the spacecraft and the RTG's was determined.

- A preliminary test program to demonstrate the effectiveness of the proposed design techniques was prepared.

B. SUMMARY

For a scientific deep-space probe with the task of measuring temporal and spatial variation in the solar wind, with its associated magnetic field, the tolerable background noise at the magnetometer should not be more than 0.1 gamma. This value represents approximately 10 percent of the average value of 1 gamma estimated for the interplanetary magnetic field at 5 AU solar distance appropriate for the NEW MOONS mission (Ref. 1 and 3). Similarly severe requirements have been imposed previously on the IMP and Pioneer programs whereby, through the use of very careful design procedures, magnetic contamination at the magnetometer was held to levels of 0.25 gamma at a separation distance of 2 meters from the spacecraft. It was assumed for the NEW MOONS study that the magnetic contamination could be held to similar levels on the GJP spacecraft, so that with RTG-magnetometer separations of the order of 4 to 6 meters the RTG magnetic contributions would become tolerable. While a 0.1 gamma noise level is probably still acceptable out to Saturn distances, missions beyond approximately 10 AU would have to assume more severe requirements. This investigation was not part of this Task but appears appropriate for further study.

A photograph of a model of the GJP spacecraft and its two cylindrical RTG's with boom-mounted detectors is shown in the frontispiece and an earlier version of this model is shown in Figure 1. Throughout this report a spacecraft of this general size and capability, i.e., 500 to 600 pounds, spin-stabilized, and consuming 100 watts (electrical) power, has been assumed.

Magnetic cleanliness techniques developed for the IMP's F and G (Ref. 5) are appropriate not only for the GJP spacecraft but also, to a certain extent, to the RTG design. Basically, these techniques consist of selecting materials devoid of magnetic properties and designing circuits, particularly those involving large currents, which avoid substantial area current loops. In addition, a comprehensive set of component magnetic tests is advocated to identify problem areas early in the design stage and to facilitate final system checkout.

In this Task, both planar and cylindrical RTG configurations have been considered. The reasons for evaluating these configurations is presented in the Task VII Report. Either configuration could be designed with PbTe or SiGe thermoelectric couples. Neither material is significant for its magnetic field contribution however, historically PbTe couples have used iron elements in the hot shoe design (SNAP-9A and-27) which do produce significant magnetic fields. Arbitrarily, for this Task, the planar generator was considered to employ the SiGe materials and the cylindrical generator the PbTe materials with iron.

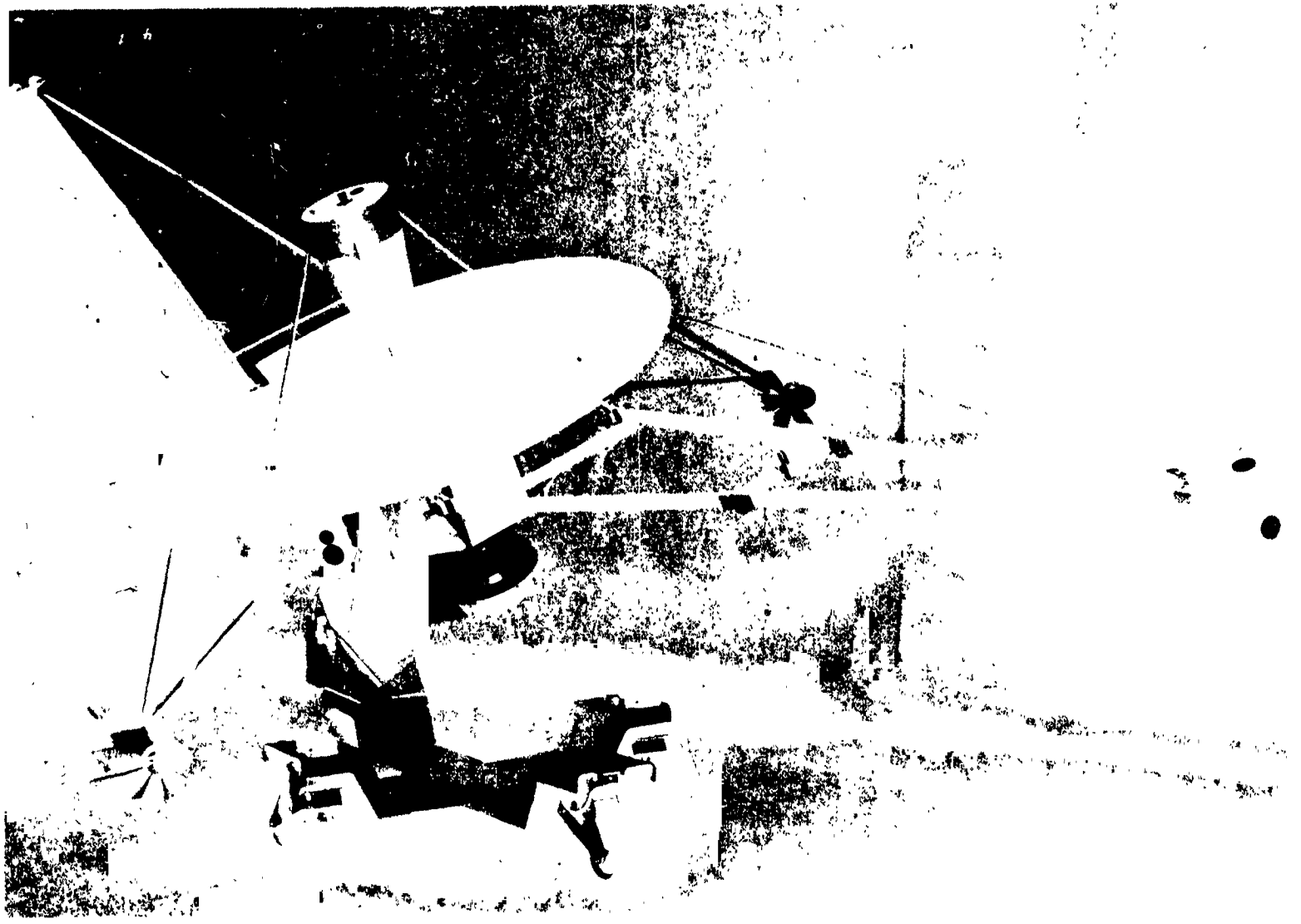

Figure 1. Preliminary Model of GJP Spacecraft with Cylindrical RTG's

The above design techniques have been evaluated for a planar RTG and a cylindrical RTG. For the planar RTG (shown in Figure 2), no magnetic material is included in the component list; consequently, the only source of magnetic contamination is the stray field associated with thermoelectric couple current loops. With the planar (SiGe) design selected for this Task, magnetic compensation is relatively simple, and, allowing for a 10-percent inaccuracy, the residual field can be reduced to the desired level at an RTG-magnetometer separation distance of 4 meters.

The cylindrical RTG (shown in Figure 3), using PbTe thermoelectric couples, was assumed to use soft iron in the region of the hot-junction. The results of testing a SNAP-27 generator using such thermoelectric couples indicated a field of 3.2 gamma at a separation distance of 6 feet (Ref. 4). Reducing this field to an acceptable level requires a separation distance (RTG-magnetometer) of approximately 7.4 meters. Replacement of the iron elements in the hot shoes by some suitable substitute material such as tungsten (this possibility was first investigated by GSFC,* then by others) would be desirable from a magnetic viewpoint. It has been estimated that the effect of such a substitution would result in a reduction, by a factor of 3, in the permanent magnetic field of the RTG. With such a reduction, the magnetic field drops to an acceptable level with a separation distance (RTG-magnetometer) of 6.3 meters.

Based on estimates for the present design of the cylindrical generator using PbTe couples with or without iron elements in the hot shoe, the effects of magnetic contamination will predominate over the effects of nuclear radiation in setting the minimum RTG-magnetometer separation distance (Ref. 6). The postulated planar generator, with SiGe thermoelectric couples, is potentially a magnetically cleaner device than the cylindrical generator, and the effects of nuclear radiation will predominate over the effects of magnetic contamination in setting the minimum separation distance of the RTG magnetometer.

In either case, testing of both the individual components and a complete generator is mandatory. Previous test procedures (Ref. 5) have advocated field mappings at half the subsystem-sensor separation distance in order for the mapping level to be at several gamma. However, with the extremely low sensor tolerance of 0.1 gamma, needed for the NEW MOONS missions, it would be more appropriate to map at one third the subsystem-sensor separation distance ($\sim$ 1 or 2 meters) to yield mapping levels of 1 or 2 gamma. If even more stringent requirements are necessary for measuring interplanetary fields, say beyond Saturn's orbit, then mapping distances would have to be reduced to maintain levels of 1 or 2 gamma.

*Epstein, J., "Segmented Thermoelectric Couples", Proceedings of 20th Annual Power Sources Conference, May 1966.

Figure 2. A Model of a Planar RTG

Figure 3. Model of Cylindrical RTG with Nuclear Shield and Attaching Hardware

The conclusion derived from the analysis for this Task is that with judicious material selection and circuit design, supported by an adequate component and subsystem magnetic test program, either the planar RTG using SiGe thermoelectric couples or the cylindrical RTG using PbTe thermoelectric couples could meet the magnetic contamination constraints imposed by the postulated scientific missions to at least Saturn's vicinity.* For missions beyond this region, where interplanetary field investigation is a prime requirement, additional studies appear appropriate.

*An order of magnitude calculation shows (Appendix I) that the spin axis of the spacecraft moves through less than 1/25 of a degree as a result of the interaction between the spacecraft magnetic field and the naturally occurring planetary and interplanetary fields during a typical Jupiter swingby mission. Correcting for this minimal spin-axis movement consumes a negligible quantity of attitude control gas, and this factor can be neglected when sizing the spacecraft's attitude control tanks.

SECTION II

REQUIREMENTS FOR MAGNETIC CLEANLINESS

A. MEASUREMENT REQUIREMENTS

The deep-space missions postulated for NEW MOONS (Ref. 1) make use of Jupiter's gravitational field to deflect the spacecraft orbit out of the ecliptic plane or to some secondary target in the plane, such as Saturn. These missions are characterized by very large solar distances (for example, 5.2 AU for Jupiter, 9.5 AU for Saturn, and beyond) and by the intended science experiments, among which the measurement of interplanetary magnetic fields is of primary importance.

The interplanetary field originates at the surface of the Sun and is "frozen in" the solar plasma. The radial expansion of the plasma combined with the rotation of the Sun results in a spiral configuration for the interplanetary field.

Measurements performed by the IMP-1 spacecraft provided a description of the boundary of the geomagnetic field and the transition to the interplanetary medium. The boundary was identified as a transition from a stable $1/r^3$ field out to 10 Earth radii in the direction of the Sun, a turbulent and rapidly fluctuating field between 10 and 15 Earth radii and a quiescent field beyond 15 Earth radii. During the time of the quiet Sun, the magnitude of the interplanetary field in the vicinity of Earth varied from 3 to 7 gamma with a time-averaged value of approximately 5 gamma.

Combining the radial and tangential components of the field as given by Ness (Ref. 2, p. 35, Equation 13, 14, and 15) its magnitude, as a function of distance from the sun, is given by

$$B = B_0 \left(\frac{r_s}{r}\right)^2 \left[1 + \left(\frac{r\Omega}{V}\right)^2\right]^{1/2} \qquad (1)$$

where

B_0 is the radial component of the magnetic field on the surface of the Sun,

r_s is the radius of the Sun,

r is the distance from the Sun,

Ω is the angular rotation of the Sun (~ 27-day sidereal period), and

V is the solar plasma streaming velocity (300 to 600 km/sec).

At the orbit of the Earth, the term $r\Omega/V$ is approximately unity so that the field is at 45 degrees to the Sun-Earth line. Since the solar-wind velocity is essentially independent of radial distance from the Sun, this term will dominate the expression at Jupiter distance; and from Equation (1) it can be seen that the magnitude of the magnetic field will be inversely proportional to r. Extrapolating the average value of the field from 5 gamma at Earth's orbit (1 AU), the expected value at Jupiter's orbit (5 AU) is 1 gamma, and at Saturn's orbit (9.5 AU), approximately 0.5 gamma. In order to monitor variations in a field of this average magnitude, the background noise at the magnetometer should not exceed 0.1 gamma (Ref. 3). This is the level taken as a goal in the present study. Extrapolation of the field to a level of 0.16 gamma at the orbit of Neptune implies a reduction in the tolerable background to 0.01 gamma. Further extrapolation is of doubtful validity since the boundary of the organized solar wind is expected to occur in the range from 10 to 100 AU.

Measurement of the interplanetary magnetic field is a primary objective of the NEW MOONS missions so that the use of deployable booms in order to provide substantial separation between the sensitive magnetometer and the spacecraft main body is an appropriate and acceptable method of achieving the desired low level of background magnetic field. In contrast, deployable booms were excluded from the Mariner design because of the secondary importance of interplanetary field measurements compared with the planetary objectives.

B. SPACECRAFT AND RTG MAGNETIC FIELD CONTRIBUTION

The magnetic fields associated with permanent and induced magnetization or circulating currents in the NEW MOONS spacecraft have been estimated on the basis of IMP F and G experience. These estimates are regarded as being the lowest levels of magnetic field reasonably attainable for the basic spacecraft with all its subsystems, excluding the RTG power sources.

Very stringent fabrication procedures were developed, as described in Reference 5, involving material selection, electronic circuit-design practices, wiring procedures, and assembly of the spacecraft structure. In addition, all subassemblies were tested for magnetic contamination prior to spacecraft integration according to a rigorous test plan and, finally, the entire spacecraft

was tested. By using these stringent methods, the desired noise level of 0.25 gamma was achieved at the magnetometer, which was located at a distance of 82 inches (~ 2 meters) from the spacecraft.

If similarly stringent design and testing procedures are employed in fabricating the spacecraft for the NEW MOONS mission, comparably low magnetic field levels should be attainable. In addition, the use of deployable booms to increase the separation distance between the sensitive magnetometer and the spacecraft structure should serve to reduce the magnetic field to tolerable levels at the magnetometer. Assuming a magnetic dipole approximation for the spacecraft (without RTG's), the IMP value of 0.25 gamma for a separation distance of 2 meters may be extrapolated to yield a spacecraft field of 0.03 gamma at 4 meters and 0.01 gamma at 6 meters; these distances are typical of the magnetometer locations envisioned for a scientific deep-space spacecraft employing planar or cylindrical RTG's, respectively. Compared with the combined spacecraft plus RTG allowable magnetic field background of 0.1 gamma at the sensor, the spacecraft contributions are quite small. The balance of 0.07 gamma and 0.09 gamma is taken to be the maximum which can be tolerated either from the two planar RTG's at 4 meters or two cylindrical RTG's at 6 meters, respectively. For a 30 AU mission, with an assumed 0.01 gamma background noise level, the required separation distances increase to 9 and 13 meters respectively. Further investigation of the magnetic measurements appropriate to missions to the vicinity of Neptune and beyond, and of the corresponding magnetic contamination tolerance, would become more meaningful after a better definition of the environment by precursor probes.

Although the magnetic cleanliness techniques employed for the IMP and Pioneer programs have been used as models for achieving tolerable magnetic cleanliness for NEW MOONS, it should be noted that neither of the above model programs incorporated the use of RTG power supplies. Though success in reducing the contamination due to the spacecraft and major subsystems may be expected by following the previously established procedures, special attention must be given to the peculiar problems associated with nuclear power sources.

SECTION III

MAGNETIC CLEANLINESS DESIGN AND TESTING CONSIDERATIONS

(For Spacecraft and Subassemblies, Brief Overview)

A. GENERAL

Previously developed design techniques for the production of magnetically clean spacecraft have been adapted to the GJP (Ref. 7 and 9). The referenced reports provide recommendations for material selection and fabrication of electronic circuits to minimize magnetic noise levels. These reports also outline acceptable magnetic testing procedures necessary to yield the desired results. It is evident from a review of this literature that it is necessary to adopt magnetic cleanliness design techniques in the early design stage to achieve a magnetically clean spacecraft to the extent required for the NEW MOONS mission. The recommended procedures are described in the following paragraphs.

B. FABRICATION AND DESIGN

1. Selection of Components for Electronic Circuits

In the design of electronic circuits for the spacecraft, the designer must avoid the use of devices that have magnetic components resulting from the presence of iron and nickel compounds. Although other materials can be magnitized, the major problem arises from the use of iron and nickel. The magnetic properties of individual components should be measured in a field-free environment to ensure their suitability. Most magnetically objectionable components have clean equivalents that can be obtained by suitable specifications. In the instance where the designer feels compelled to use a magnetically unsuitable component, the overriding consideration must be the magnitude of the effect on the specified tolerance level, since exceeding this level will only serve to defeat the initial design objective pertaining to magnetic cleanliness.

2. Selection of Materials for Structural Components

All structural members, including nuts, bolts, etc., should be of non-magnetic material. Generally, aluminum and magnesium are magnetically clean, although care must be taken in working these materials with tools that may leave a residue of magnetic chips. Lists of non-magnetic materials and preferred parts are provided in Reference 8.

3. Wiring Techniques

For interconnections between densely packed assemblies, the use of alloy-180 welded wire work is recommended. No nickel ribbon or nickel alloys such as rodar should be used. All leads carrying appreciable currents (tens of milli-amperes) should be bifilar wound so as to self-cancel magnetic effects.

Component leads are frequently a source of contamination, that can be minimized by trimming all such leads to not more than 0.25 inch when the components are mounted.

The heavy leads from a power supply should be wired with extreme care to assure cancellation of stray magnetic fields. Preferably, such wiring should provide cancellation on a modular basis so that failure of separate modules will not distort the overall current-flow pattern.

4. Design Techniques for Reducing Magnetic Contamination at Magnetic Field Detector

The use of long booms to locate the sensitive magnetometer at a suitable distance from the RTG and from the spacecraft structure is an appropriate and acceptable method of reducing magnetic contamination for a spacecraft with primary interplanetary scientific objectives. As a practical spacecraft design matter, complete reliance on the $1/r^3$ dependence of the field due to a dipole is not advisable, because the use of very long booms adversely affects spacecraft dynamics. For the NEW MOONS missions, it is likely that the spacecraft will also carry radiation sensors. These sensors will be adversely affected by neutron and gamma radiation emanating from the RTG and will require the combined techniques of remote location (booms) and radiation shielding if the background radiation at the sensors is to be reduced to a tolerable level. Attempts to minimize the weight of booms and shields, together with constraints on magnetic contamination and spacecraft dynamics, lead to the preferred magnetometer and radiation detector separations described in Reference 6.

At this time, the use of magnetic shielding is not recommended for the NEW MOONS missions (Ref. 7, p. 11). *Shielding is only appropriate for reducing the

*Dr. J. Trainor of GSFC has recently completed the development of a magnetic shield as the envelope of a detector whose purpose it is to discriminate particle energy. The discrimination is done by a horseshoe permanent magnet whose magnetic field is in the order of a 1000 gauss with a pole separation of 1 cm. Extemal to the detector, with the shield in place, the magnetic field is within GJP, SSS, and IMP spacecraft specifications. The shield is made of a cobalt-nickel alloy fabricated and handled in a very special (proprietary) manner. While a few assemblies have been made and tested, additional long-term environmental tests are planned. However, many physical shock tests at room temperature have been performed, and subsequent measurements have shown stability of the shield's magnetic behavior. This promising development will be watched with interest for application to specific problem areas.

effects of physically small permanent magnets. Similarly, attempts to cancel inherent spacecraft dipoles by introducing compensating permanent magnets or bucking coils depends on the invariance of the source (and compensation) and is not compatible with the very low magnetic field background which is required in this application.

C. SUBASSEMBLY TESTING PROCEDURES FOR MAGNETIC CONTAMINATION — FOR OTHER THAN RTG's

The problem of spacecraft magnetic contamination becomes vastly more difficult if individual problem areas are not treated separately, before spacecraft integration. It is recommended that all logically distinct subassemblies should be individually tested according to the following sequence and criteria:

1. Test Environment

All magnetic measurements should be made in a field-free environment, requiring cancellation of the Earth's magnetic field to an accuracy of 1 gamma.* Test of the initial, post-exposure, post-deperm, and stray magnetic fields shall be made on all subassemblies as prescribed in the preliminary test plan described in Section V.

2. Initial Permanent Magnetic Field

The equivalent dipole magnetic moment shall be determined by mapping the magnetic field of the subassembly over a spherical surface at both 18 and 36 inches from its geometrical center. The maximum allowable field is 8 gamma at 18 inches or 1 gamma at 36 inches, if a dipole representation is valid.

3. Post 25-Gauss Exposure

Similar measurements to those made for the initial magnetic fields shall be performed after the subassembly has been subjected to a 25-gauss field along the direction of the initial magnetic moment. The purpose of this test is to determine the maximum extent to which the subassembly could become magnetized during dynamic testing or during the launch maneuver. The maximum allowable field is 32 gamma at 18 inches, or 4 gamma at 36 inches.

4. Post 50-Gauss Deperm

A deperming process, consisting of exposure to a steadily decreasing alternating field, is used to reduce the permanent field to a minimum level. Mapping

*See Section V for a description of Goddard's Magnetic Test Facility's Capabilities

at 18 and 36 inches is again required with tolerable levels of 2 gamma and 0.25 gamma, respectively.

5. Stray-Field Mapping

The stray field is the difference between "power-on" and "power-off" conditions. Mapping at 18 and 36 inches is used to determine the characteristic of the stray field. The maximum allowable stray fields are 4 gamma and 0.5 gamma, respectively.

The test conditions, distances, and the acceptable levels for the NEW MOONS subassemblies are summarized in Table 1.

Table 1

Criteria For Testing Subassemblies For Magnetic Contamination*

Test Condition	Max Magnetic Field (Gamma)	
	18 in.	36 in.
Initial perm	8	1
Post 25-gauss exposure	32	4
Post 50-gauss deperm	2	0.25
Stray field ("Power-on" minus "Power-off")	4	0.5

*For all subassemblies except RTG; however, it could be an RTG-design goal

D. SPACECRAFT TESTING PROCEDURE FOR MAGNETIC CONTAMINATION

The spacecraft, as defined for magnetic testing, contains the structure and all subsystems, both mechanical and electrical, except the RTG power source. The stringent fabrication and material selection procedures which apply to subassemblies and subsystems are equally appropriate for the integration of the subsystems to the spacecraft. It is necessary that the spacecraft be tested in this condition to ascertain the effectiveness of the integration procedures.

As previously noted, compelling reasons may exist to use subassemblies which have magnetic fields greater than the levels specified as "criteria" in Table 1. The testing of the spacecraft in this condition can establish the extent to which these "non-complying" subassemblies contribute to the magnetic field production of the spacecraft. Decision on the acceptability of these subassemblies can then be made at this level.

The spacecraft is taken to be magnetically acceptable if, in an operating condition, it can be represented as a dipole with maximum magnitude 0.25 gamma at a distance of 2 meters. To ensure that these objectives are met, the spacecraft should be tested to the sequence described in paragraph C, but to the criteria described in Table 2.

Table 2

Criteria For Testing A Spacecraft (Without RTG)
For Magnetic Contamination

Test Condition	Max Magnetic Field (Gamma) at 36 in.
Initial perm	1.0
Post 25-gauss exposure	10.0
Post 50-gauss deperm	1.0
Stray field ("Power-on" minus "Power-off")	1.0

E. POST SPACECRAFT ASSEMBLY CONSIDERATIONS

Following the final assembly of the spacecraft a number of environmental factors must be considered, all of which may affect the behavior of the measured magnetic performance of the spacecraft. Such factors as final acceptance testing, shock due to transportation to the launch site, vibration and shock due to the launch sequence, and the exposure of the spacecraft to the Earth's magnetic field, must be considered. Accordingly, it has been assumed for this Task that the Initial Perm criterion plus the stray field represents the magnetic characteristic of the spacecraft and has been used in developing the design curves of Section IV.

SECTION IV

EVALUATION OF RTG DESIGN TECHNIQUES RE: MAGNETIC CLEANLINESS

A. TECHNICAL APPROACH

The fabrication and testing procedures outlined in Section III must be rigidly applied in order for the integrated spacecraft to meet the overall requirement for magnetic cleanliness. Similar design techniques must be employed for the RTG power sources, particularly in the selection of suitable materials and in the elimination of current loops in a system where large currents are obviously to be encountered and which contribute adversely to its magnetic performance. However, instead of applying the subassembly testing criteria to the RTG's, it may be more reasonable to attempt to reduce the spacecraft-less-RTG-field to the IMP level (0.25 gamma at 2 meters) and to allocate the balance of the specified 0.1 gamma level (at the magnetometer) to the RTG's.

The two candidate RTG designs considered in this Task make use of these cleanliness techniques to differing extents, and estimates have been made of the magnetic field which each will generate. Reasonable levels are 0.03 gamma at 4 meters for the planar (SiGe) RTG, and 0.046 gamma at 6.3 meters for the cylindrical RTG using PbTe couples without iron in the hot shoes.

For stray-field evaluation, it was arbitrarily assumed that the output voltage of a planar RTG is of the order of 7.5 volts*, thereby generating 10 amperes of current for the case of a 75-watt generator. The cylindrical RTG on the other hand was evaluated at its expected operational level of 4 amperes. (Ref. 4.)

B. EVALUATION OF PLANAR RTG WITH SiGe THERMOELECTRIC ELEMENTS

The materials from which the components of a 75-watt end-of-life planar RTG will be manufactured are listed in Table 3. None of these materials is magnetic, that is, each has a permeability of less than 1.02 at the temperature at which it will operate. In addition to the fundamentally acceptable material selection, tests have been performed on similar RTG components with satisfactory results (Ref. 4), in particular SNAP-27 beryllium radiator, SNAP-9A

*In general, a higher voltage (lower current) RTG is preferred for magnetic reasons.

Table 3

Materials List for Planar RTG*

Component	Material	Estimated Weight (lb)	Estimated Operating Temperature (°F)
Fuel Capsule	Pu^{238} O_2	13.6 (Encapsulated wt.)	1725
	Haynes-25 Container	5 lb. for Haynes-25	
	Ta-10W-liner	1 lb. for liners	
T/E Elements (112)		5.04 (Module wt.)	
Hot Shoe	Si Mo		1490
N Element	Si Ge		500-1450
P Element	Si Ge		500-1450
N Cold Shoe	Tungsten		500
P Cold Shoe	Tungsten		500
N Pedestal	OHFC Cu		500
P Pedestal	OHFC Cu		500
N Compensator	Tungsten		500
P Compensator	Tungsten		500
Electrical Connector	Cu		500
Spacer	Alumina Ceramic		475
Disc	Cu		475
T/C Mounting Stud	Be		475
Foil Insulation	Pt-Micro-Quartz	3.78	500-1650
Radiator	Be	17.26	450
Heat Shield	Pyrolytic Graphite	8.93	470
Basket		5.95 (Total)	
Inner	Haynes-25		1670
Outer	Haynes-25		

*75 watt (electrical) End-of-life

fuel capsule, and SNAP-17 SiGe thermoelectric material. Neither the suitability of the basic material nor previous test results, however, preclude individual testing of the components for the NEW MOONS planar generator, although they do give reasonable assurance that there is no essential flaw in the preliminary material selection.

The predominating source of magnetic field in the planar RTG is current loops in the thermoelectric element circuitry. One possible thermoelectric element electrical circuit is illustrated in Figure 4. The residual dipole moment of these loops is given by the vector sum of the individual loop dipoles. Each vector is normal to the plane of the loop and its magnitude is equal to the product

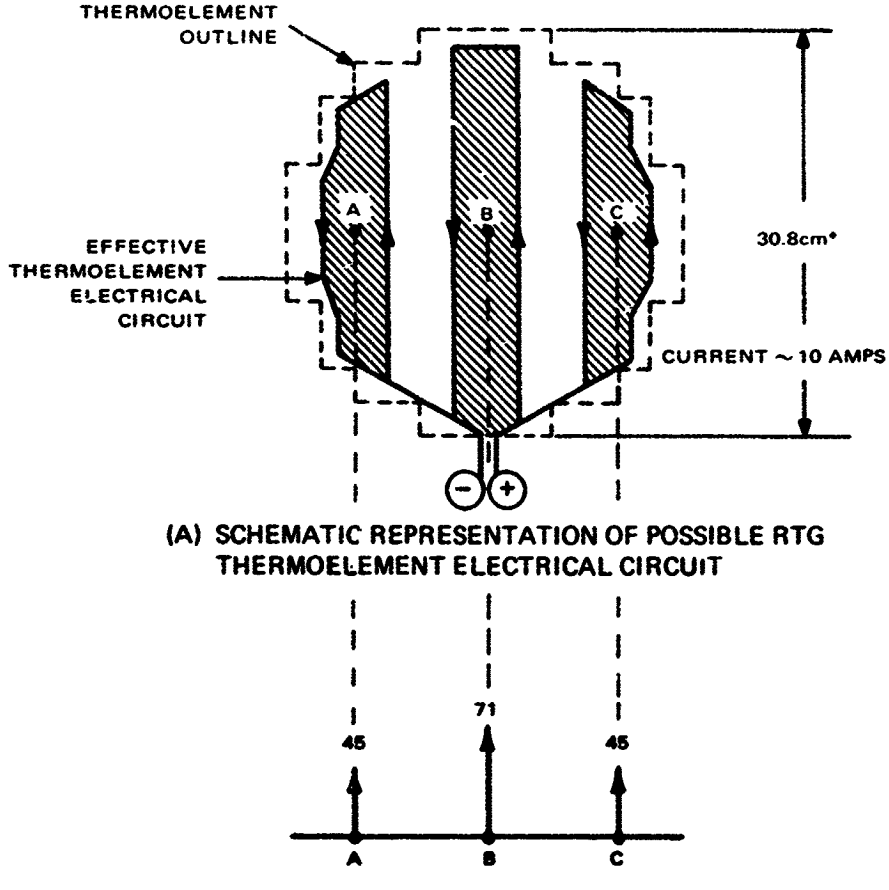

Figure 4. Possible RTG Thermoelectric-element Electric Circuit Configuration with Corresponding Dipole Moments

of the current and the enclosed area. With the current, I, in amperes and area, A, in square centimeters, the dipole moment is given by $\frac{IA}{10}$ pole-cm. The moments corresponding to the circuit in Figure 4 (A) are shown in Figure 4 (B), and the effect at distances large, compared with the circuit dimension, is substantially that of a single magnetic dipole of magnitude 161 pole-cm.

The radial and tangential components of the magnetic field due to a dipole of moment, M, at a point with polar coordinates r, θ are

$$B_r = 2M \cos\theta/r^3$$

$$B_\theta = M \sin\theta/r^3 \qquad (2)$$

where θ is the angle between the dipole axis and the radius. Combining these components, the magnitude of the field at r, θ is

$$B = \frac{M}{r^3}(1 + 3\cos^2\theta)^{1/2} \qquad (3)$$

Thus, the field due to the 161 pole-cm dipole at a distance of 1 meter normal to the axis is 161×10^{-6} gauss or 16.1 gamma, and decreases as r^{-3}.

By suitably rewiring the thermoelement circuit, the current loops can be arranged to give a zero net dipole. One suggested arrangement is shown in Figure 5 (A) where the four enclosed areas form two pairs of dipoles of equal magnitude and opposite polarity as shown in Figure 5 (B). The net dipole moment of this arrangement is effectively zero, though higher order effects do exist. Two equal and opposite dipoles of magnetic moment M, separated by a distance, d, yield a quadrupole field with components as illustrated in Figure 6. For the two pairs of matched dipoles in Figure 5 (B), the resultant quadripole moment is given by

$$\Sigma M_d = 145 \times 10.28 - 50 \times 27.8 = 100 \text{ pole-cm}^2 \qquad (4)$$

and the magnitude of the coefficient 3 (M_d/r^4) is 0.3 gamma at 1 meter, and decreases as r^{-4}. The effect of the quadrupole and of higher-order multipoles,

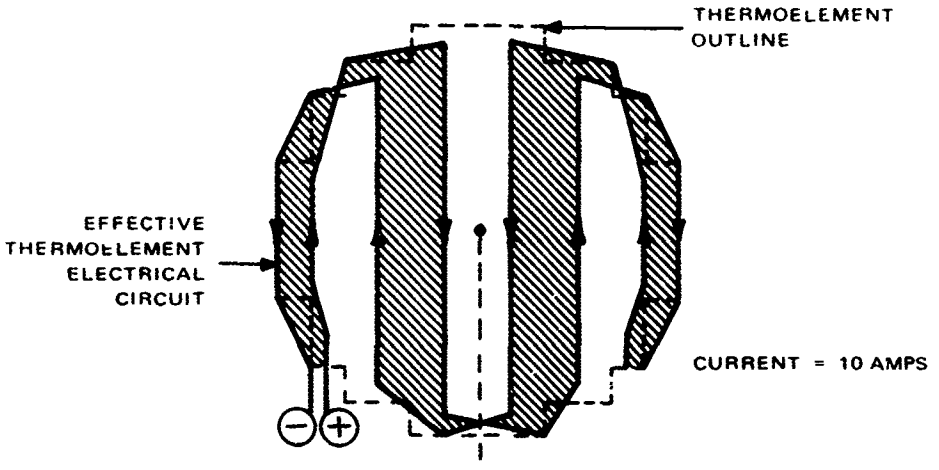

(A) SCHEMATIC REPRESENTATION OF SUGGESTED RTG THERMOELEMENT ELECTRICAL CIRCUIT

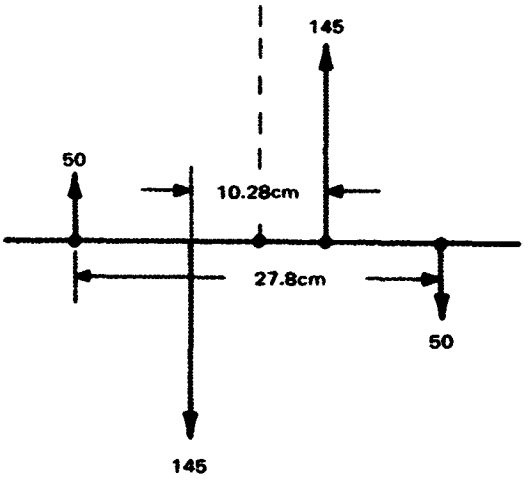

(B) EQUIVALENT MAGNETIC DIPOLES (POLE-CMS)

Figure 5. Suggested RTG Thermoelectric-element Electrical Circuit Configuration with Corresponding Dipole Moments

then, is very small at distances of interest to this study and the major source of contamination is likely to be residual dipole fields due to inaccurate cancellation. The magnitude of the fields, due to the uncompensated loops of the configuration shown in Figure 4, due to a 90-percent compensated loop similar to that shown in Figure 5, and due to the quadrupole of Figure 6, are plotted against RTG-sensor separation in Figure 7. The RTG allowance is calculated on the assumption that the NEW MOONS spacecraft produces a dipole field of magnitude 0.25 gamma at 2 meters. Extrapolating this value to 3 meters yields a spacecraft field of 0.08 gamma so that the maximum contribution which can be tolerated

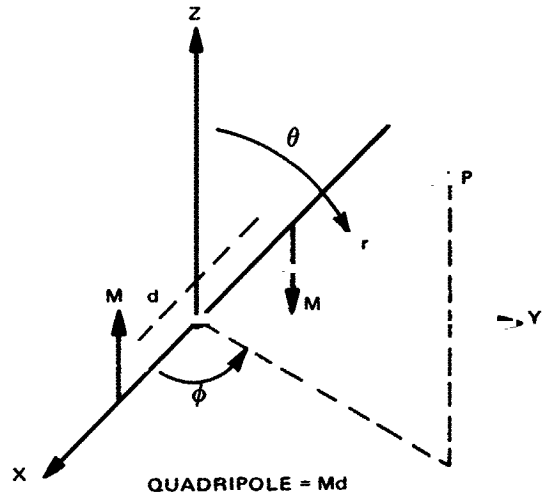

QUADRIPOLE = Md

$$B_r = -\frac{9}{2}\left(\frac{Md}{r^4}\right) \text{SIN } 2\theta \cos\phi$$

$$B_\theta = 3\left(\frac{Md}{r^4}\right) \cos 2\theta \cos\phi$$

$$B_\phi = -3\left(\frac{Md}{r^4}\right) \cos\theta \text{ SIN}\phi$$

$$B_{MAG} = 3\left(\frac{Md}{r^4}\right)\left\{\cos^2\phi\left[\frac{5}{4}\text{SIN}^2 2\theta + 1\right] + \text{SIN}^2\phi\cos^2\theta\right\}^{1/2}$$

Figure 6. Magnetic Field of a Quadrupole

from each RTG is 0.01 gamma, assuming worst-case addition of the fields at the sensor. The RTG allowances for various separation distances are summarized in Table 4.

Table 4

Planar RTG Magnetic Field Allowance for Several Separation Distances

Separation Distance (meters)	Magnetic Field (gamma)		
	Spacecraft	Allowance for 1 RTG	Total
3	0.08	0.01	0.1
4	0.03	0.035	0.1
6	0.01	0.045	0.1

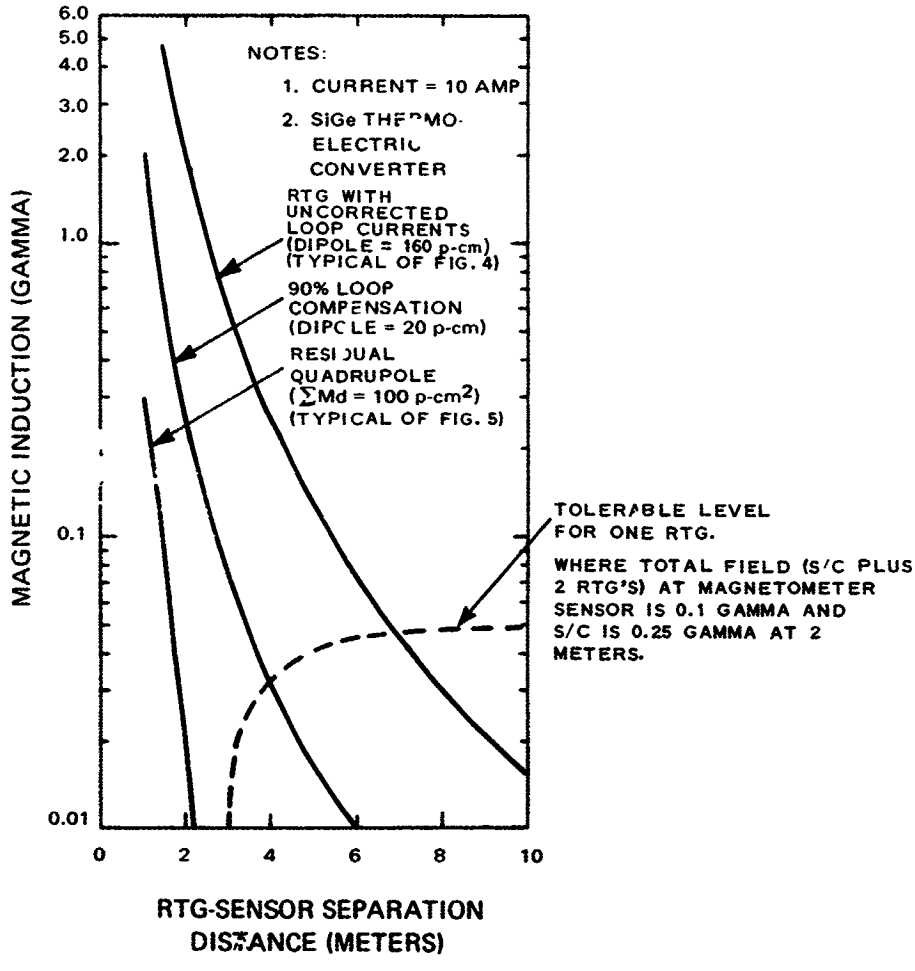

Figure 7. Planar RTG-Sensor Separation Distance as a Function of Magnetic Induction

It can be seen from Figure 7 that the quadrupole field is negligible and the effect of the RTG could be ignored if this were a valid representation. The uncorrected current-loops dipole effect, on the other hand, requires a 7-meter separation before its contribution is tolerable. Current-loop compensation to 90-percent accuracy should not be too difficult in this situation and is regarded as the most reasonable estimate for the planar generator design. Thus, a 4-meter RTG-magnetometer separation appears adequate; this situation is illustrated in Figure 8 for the worst-case combination of the spacecraft plus two RTG's reaching the sensor noise level of 0.1 gamma at 4 meters separation.

C. CYLINDRICAL RTG WITH PbTe THERMOELECTRIC ELEMENTS

A modified version of the SNAP-27 generator has been proposed as a possible power source for the NEW MOONS missions and an estimate of its

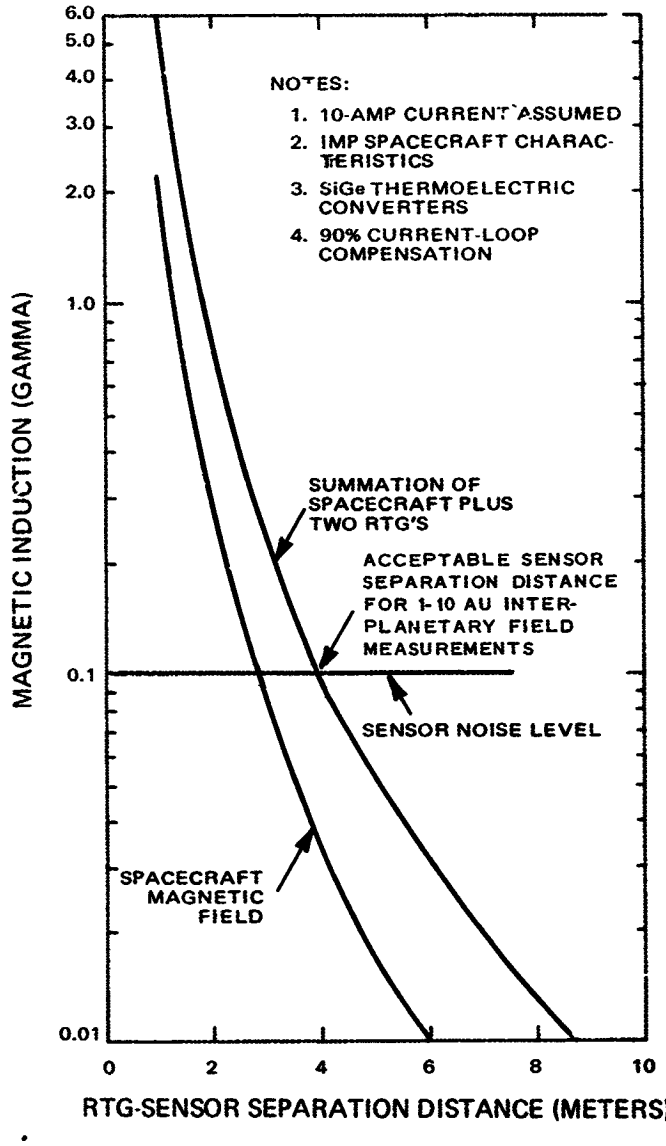

Figure 8. Magnetic-Field Produced by a Spacecraft Plus Two Planar RTG's

magnetic properties is provided in Reference 9. Magnetic-field measurements of the SNAP-27 Model 8B, performed at Goddard Space Flight Center (Ref. 4) are summarized in Table 5.*

From these test results it is estimated that, under typical operating conditions, of interplanetary flight, the RTG-induced field at 6 feet will be 3.2 gamma. This is based on 2.1 gamma perm (which is taken as representative of the effect on a previously depermed generator being exposed to the Earth's field and other factors noted in Section III) plus 1.1 gamma due to stray fields. At 6 meters separation (minimum weight configuration, see Reference 6), the field reduces to

*The relevant portion of Reference 4 which deals with SNAP-9A and SNAP-27 is given in Appendix II. Recent test data for SNAP-19 are given in Appendixes III, IV and V.

Table 5

SNAP-27 Magnetic Field Test Results

Test Condition	Magnetic Field (Gamma)	
	3 ft	6 ft
Initial perm	20	2.1
Post-15-gauss exposure	59.4	6.4
Post-50-gauss deperm	0.2	0.2
Stray field (determined at 4 amp)	8.5	1.1

0.09 gamma, approximately equal to the combined spacecraft plus two-RTG allowance of 0.1 gamma at the sensor. Further extrapolation to 7.4 meters is necessary before the RTG field is sufficiently low (0.046 gamma) to satisfy the NEW MOONS magnetic constraints.

To achieve such large RTG-magnetometer separations require very long booms which if avoidable, are undesirable from a weight consideration and also lead to poor spacecraft inertia ratios. In order to improve the situation with regard to boom length, the basic cause of the problem, the iron used in the hot shoes of the SNAP-27 design, should be replaced by a suitable non-magnetic material. Development of tungsten shoes as an alternative is being carried out (Ref. 10). The net effect of the iron has been estimated to be a factor of 3 increase in the permanent magnetic field components over operation with non-magnetic materials (Ref. 4). Replacement of the iron then could reduce the magnetic field at 6 meters from 0.09 gamma to approximately 0.05 gamma and the RTG field falls to an acceptable level at a separation distance of 6.3 meters, as shown in Figure 9. This has been taken as a reasonable goal for a magnetically clean version of the SNAP-27 generator to be used for interplanetary measurements to 10 AU, and it yields a suitable solution to the weight/spacecraft-inertia combination. The magnetic fields due to the spacecraft alone, and worst-case combinations of spacecraft plus two SNAP-27 RTG's of the type tested at GSFC are illustrated in Figure 10.

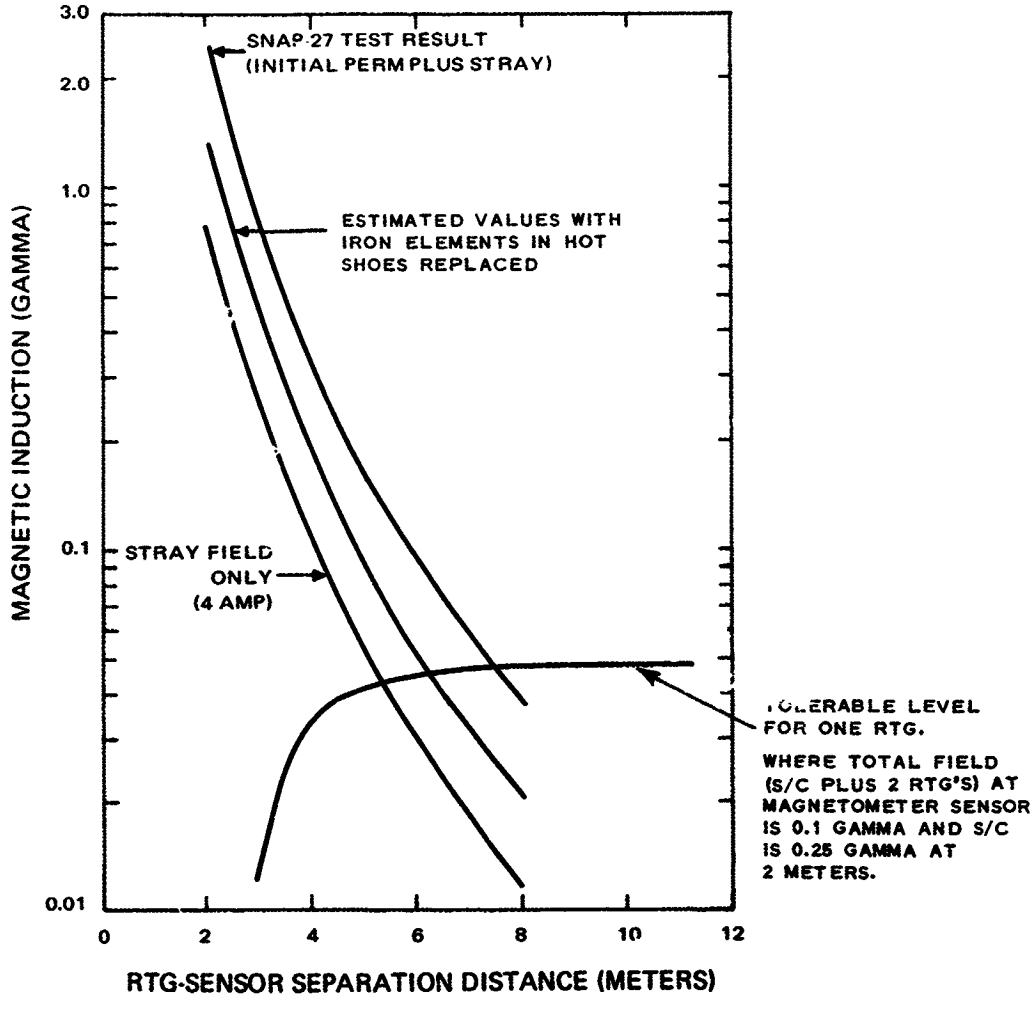

Figure 9. Magnetic Field of Cylindrical RTG Using PbTe Thermoelectric Couples

D. SPACECRAFT-PLUS-RTG EVALUATION OBJECTIVES

The design objective for the integrated spacecraft, including its RTG power sources, is a noise level not exceeding 0.1 gamma at the magnetometer. The estimate of operational condition is again taken to be the sum of initial perm plus stray-field contributions. Mapping should be carried out so that fields of 1 gamma are accurately predicted. Measurement at one-third the magnetometer-spacecraft separation at a level of 1 to 2 gamma should provide this sensitivity. The validity of a dipole approximation to the spacecraft field can then be checked by measurements performed at half the magnetometer-spacecraft separation. Measurements made at one-half distance (~2 meters for the planar RTG and 3 meters for the cylindrical RTG) will be less susceptible to anomalies, due to

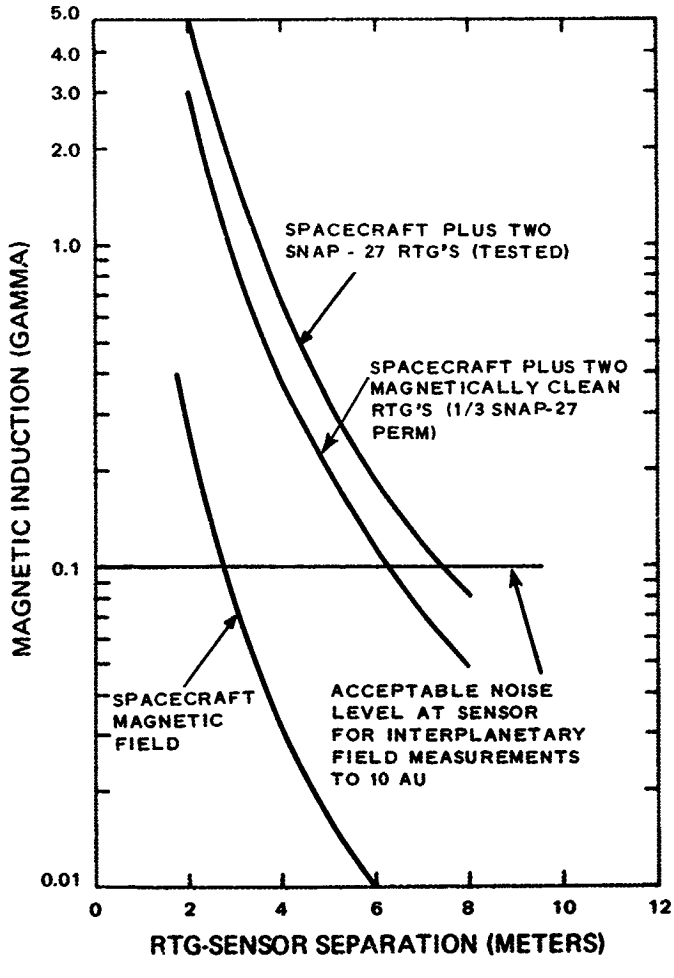

Figure 10. Magnetic Field Produced by Spacecraft Plus Two Cylindrical RTG's

the large physical size of the spacecraft, and will allow reasonable prediction of the overall field at the sensor location.

For the integrated spacecraft the test conditions described for subassemblies shall be used with the test criteria shown in Table 6.

E. CONCLUSIONS

Magnetically clean designs, suitable for the selected NEW MOONS mission, of either cylindrical or planar RTG's appear possible if the stringent material selection, fabrication, and testing procedures outlined in this Task are followed. Previously tested SiGe thermoelectric couples have an advantage over generally

Table 6

Postulated Criteria For Integrated Spacecraft* Plus Two RTG's
(For Interplanetary Field Measurements of ~1 to 10 AU)

Condition	Maximum Magnetic Field (Gamma)	
	1/3 (S/C-Magnetometer Separation)	1/2 (S/C-Magnetometer Separation)
Initial perm	1.4	0.4
Post-25-gauss exposure	1.7	5.0
Post-50-gauss deperm	1.4	0.4
Stray field ("Power on" minus "Power-off")	1.4	0.4

*See References 3 and 6

used PbTe couples, which employed iron in the hot shoes, in easing the problem of magnetic contamination due to the total absence of magnetic material in the design. Loop compensation may also be easier to achieve with the SiGe planar design due to the simpler geometrical arrangement of the thermoelectric circuits. The SNAP-27 results for stray fields due to 4-ampere currents are approximately four times those estimated for the planar RTG (90-percent compensation) using 10-ampere currents. The details of the magnetically acceptable spacecraft-RTG combinations are summarized in Table 7.

Table 7

Postulated Criteria For Spacecraft-RTG Combinations
(For Interplanetary Measurements of ~1 to 10 AU)

RTG Type	RTG-Sensor Separation (Meters)	Magnetic Field (Gamma)		
		Spacecraft†	One RTG†	Σ Max
Planar, SiGe material	4.0	0.034	0.032	0.1
Cylindrical, PbTe material	6.3*	0.008	0.046	0.1

*Assuming reduction of permanent magnetism to a third of SNAP-27 values by removal of iron elements from the PbTe thermoelectric-couples hot shoes

† Contribution to magnetic field at the sensor, assuming the stated RTG-sensor separation distance

SECTION V

PRELIMINARY TEST PLAN

A. GENERAL

In order to demonstrate the effectiveness of the design techniques which have been described, and to validate the theoretical predictions of a suitably low magnetic field, the RTG's must be adequately tested prior to integration with the spacecraft. The test procedure to be followed should parallel that outlined in Section III, paragraph C, and described in more detail in References 5 and 7. This is applicable to complete spacecraft and/or subsystems. The test criteria should be modified from that applied to other spacecraft subassemblies, however, to reflect the significance of the RTG's. The test criteria should be compatible with an operational field magnitude of 0.032 gamma at 4 meters for the planar RTG and 0.046 gamma at 6.3 meters for the cylindrical RTG.

Each of the major subassemblies of the RTG's, such as, the fuel capsule, thermoelectric elements, insulation, radiator heat shield, and baskets should be tested individually to identify potential problem areas before RTG integration. Testing of these components and of the complete RTG requires the following test facilities:

(1) A controlled environment with a coil system for nulling the Earth's field to an accuracy of 1 gamma,

(2) Motion fixtures including a gimbal system for rotation and a carriage for translation, and

(3) Exposure fields such as perm-deperm coils and rotating fields.

The Goddard Space Flight Center facilities meet those requirements and have been used as a model for this test plan.

B. GODDARD SPACE FLIGHT CENTER TEST EQUIPMENT

1. Attitude Control Test Facility

a. Sixty-foot non-magnetic building with a forty-foot coil system for nulling the Earth's field

b. Nine-foot perm-deperm coils

c. Three-ton electric hoist

d. Dolly and track

e. Three triaxial fluxgate probes

2. Operations and Instrumentation Building

a. Electronic controls for coil system

b. Earth's field monitor and compensation system

c. Artificial field control for calibration

d. High power control for d-c perm and a-c deperm functions

e. Three Forster/Hoover FM 5050 magnetometers

f. Nine channels of analog strip recorders

g. Slow-speed digital printers

h. High-speed digital acquisition system (MADAS)

C. TEST PREPARATION

The following general procedure is recommended for preparing the test facility and the test object for magnetic-field testing.

1. Test Facility

a. Activate the facility coil system to null the Earth's magnetic field to zero along each axis. Verify this by inverting a fluxgate probe 180° at the center and noting the deflection.

b. Check the magnetic-field gradient at three feet from center with a probe; compensate, if necessary.

c. Position the three triaxial probes with their axes parallel with the facility's coil axis. Position one at five feet north on the anticipated centerline of the object to be tested. Position the second on the same centerline at ten feet north. Position the third five feet directly above the object.

d. Check the calibration of all magnetometers and recorders. Null all probes to zero.

2. Test Object

a. Precise handling procedures of the test object will be determined prior to the actual test as those will be dependent on the object.

b. The last step of object preparation will be the mounting of the device to the top surface of the wood turntable which is part of the facility's 5000-pound test dolly.

D. MAGNETIC-FIELD TESTING

1. Initial Perm

a. Roll the dolly along the track to the center of the facility and lock the wheels. Record "out" versus "in" effect as soon as all personnel have cleared the test area.

b. Using remote control, rotate the turntable clockwise two turns at 1/2 rpm while recording magnetometer readings with the slow-speed digital printer and analog recorders.

c. Rotate the turntable clockwise two turns at one rpm, while recording magnetometer readings with the high speed MADAS and analog recorders.

2. Post 25-Gauss Exposure

a. Rotate the test object until the maximum initial moment lies parallel to the axis of the nine-foot perm coils. Apply a d-c field of 25 gauss.

b. Obtain rotational data as before.

3 Post 50-Gauss Deperm

a. Apply a 50-gauss, 60-Hz a-c field and diminish the field slowly to zero, while rotating the device at 5 rpm.

b. Obtain rotational data as before.

c. Obtain "in" versus "out" data by removing the test object and dolly from the test area.

4. Induced Moment

a. Apply a field of 30,000 gamma along the north direction, and null all probes to zero.

b. Return the test object and dolly to the center of the facility.

c. Obtain "out" versus "in" data as soon as personnel have cleared the test area.

d. Obtain rotational data as before.

e. Reduce the applied magnetic field to zero and repeat the rotational measurement.

5. Stray Field (Applicable if Circuit is Present)

a. Connect power cables to the device.

b. Make field measurements at several current values and record data in "power-on" and "power-off" modes.

LIST OF REFERENCES

1. "Analysis of Selected Deep-Space Missions," NEW MOONS Task I Report, X-701-69-170, GSFC.

2. Ness, Norman F., "Theoretical Model of the Interplanetary Medium" Introduction to Space Science, Gordon and Breach (1965).

3. Sonnet, Charles P., "Recommendations of the Particles and Fields Subcommittee in Relation to Magnetic Spacecraft," JPL Tech. Memo No. 33-216, Proceedings of the Magnetic Workshop, JPL, (March 30 - April 1, 1965).

4. Epstein, J., D. W. Harris, and W. S. West, "Advanced Nuclear Systems Study," X-716-67-323, GSFC, (July 1967).

5. Ness, Norman F., "Magnetic Field Restraints for IMP's F and G," X-672-64-197, GSFC, (July 9, 1964).

6. "Weight Minimization Study," NEW MOONS Task IV Report, X-701-69-174, GSFC.

7. "Magnetic Field Restraints for a Small Galactic Jupiter Probe," GSFC, (August 1965).

8. Bastow, J. G., (ed.), "Proceedings of the Magnetics Workshop," JPL TM 33-216, (September 1965).

9. "Galactic Jupiter Probe," Phase A Report, X701-67-566, GSFC, (November 1967).

10. Weinstein, M., F. Wald, and W. E. Bates, "The Bonding of Lead Tulleride with Non Magnetic Electrodes," AIAA/IEEE Thermoelectric Specialists Conference, (May 17-19, 1966).

11. Magnetic Field Restraints for Spacecraft Systems and Subsystems X-325-67-70, February 1967, by Chuck A. Harris, C. Leland Parson and Norman F. Ness.

APPENDIX I

INTERACTION BETWEEN SPACECRAFT'S AND NATURALLY OCCURRING MAGNETIC FIELDS

An order-of-magnitude calculation was made to determine the angular displacement of the spacecraft spin vector as a result of interaction between the spacecraft's magnetic field and the planetary (Earth and Jupiter) and interplanetary magnetic fields for a 1300-day flight. This calculation indicates that the displacement angle is negligible and a refined calculation not warranted for this study. The magnetic field interaction effect can be neglected with regard to sizing of the attitude control gas requirements. While the following calculations were made for a spacecraft using planar RTG's (SiGe thermocouples), a similar and negligible displacement angle would result were the spacecraft to employ cylindrical RTG's (PbTe thermocouples):

1. The magnetic torque is

$$\bar{T} = \bar{M} \times \bar{B}$$

2. Magnetic dipole of spacecraft using planar RTG(s)

, Magnetic field is 0.1 gamma at 4 meters and,

$$\bar{M} = 10^{-6} (400)^3 = 64 \text{ dyne cm/gauss}$$

3. Magnetic field environment

   a. Near Earth, $\bar{B} = 0.3$ gauss at equator

   Trajectory

   After 1 hour, 6.6 R_E

$$\text{field} = 0.3 \left(\frac{1}{6.6}\right)^3 = 1.04 \times 10^{-3} \text{ gauss}$$

After 5.5 hours, 33.5 R_E

$$\text{field} = 0.3 \left(\frac{1}{33.5}\right)^3 = 8 \times 10^{-5} \text{ gauss}$$

b. Interplanetary — from 40 R_E to 40 R_J

$$\text{field, } \bar{B} = 5 \times 10^{-5} \text{ gauss}$$

c. Near Jupiter, $\bar{B}$ = 1 gauss at 3 R_J

Trajectory

Closest approach = 8.4 R_J

$$\text{field} = 1 \times \left(\frac{3}{8.4}\right)^3 = 0.59 \text{ gauss}$$

5 hours before and 5 hours after closest approach, 10 R_J

$$\text{field} = 1 \times \left(\frac{3}{10}\right)^3 = 0.27 \text{ gauss}$$

1.5 days before and 1.5 days after closest approach, 30 R_J

$$\text{field} = 1 \times \left(\frac{3}{30}\right)^3 = 10^{-3} \text{ gauss}$$

Table I-1 summarizes the trajectory, magnetic field, and magnetic torque produced by interaction of spacecraft and environmental magnetic fields.

4. Spacecraft moment of inertia about the thrust axis is

I_z = 250 slug-ft^2 or 3.3 × 10^9 gm-cm^2.

Table I-1

Magnetic Torque

	Time	R	$\bar{B}$, Field	$\bar{T}$, Torque
Earth Environment	0	1 R_E	0.3 gauss	19.2 dyne-cm
	1 hr.	6.6 R_E	0.001	6.4×10^{-2}
	5.5 Hrs.	33.5 R_E	8×10^{-5}	5.1×10^{-3}
Interplanetary	550 days	40 R_E - 40 R_J	5×10^{-5}	3.2×10^{-3}
Jupiter Environment	-1.5 days	30 R_J	10^{-3}	6.4×10^{-2}
	-5 hours	10 R_J	0.027	1.73
	0*	8.4 R_J	0.059	3.84
	+5 hours	10 R_J	0.027	1.73
	+1.5 days	30 R_J	10^{-3}	6.4×10^{-2}
Post Encounter	700 days		5×10^{-5}	3.2×10^{-2}

*Time of closest approach to Jupiter

5. Angular momentum of the spacecraft (at 3 RPM spin rate)

$$H = I\omega = 1.04 \times 10^9 \text{ gm-cm}^2 \text{ sec}^{-1}.$$

6. Torque $\bar{T} = \frac{d\bar{H}}{dt} = \bar{\Omega} \times \bar{H}$

where $\bar{\Omega}$ is the precession, rad/sec

$$\Omega = T/H$$

$$\Delta\theta = \int \omega \, dt = \frac{\int T \, dt}{H}$$

where $\Delta\theta$ is the precession angle, rads.

A torque-time curve for the flight is shown in Figure I-1.

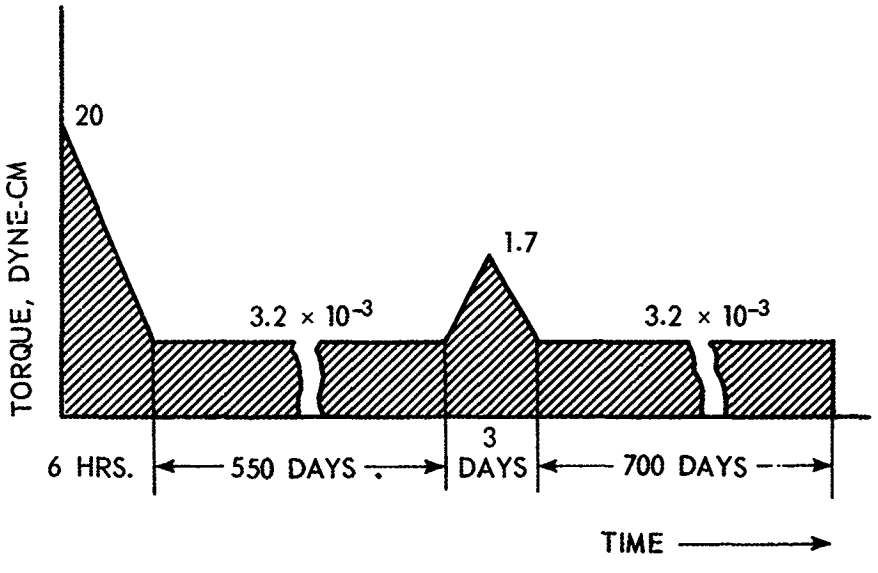

Figure I-1. Torque-Time Curve

7. $\int T \, dt$ = is the area under the curve of Figure I-1

and is 766×10^3 dyne-cm-sec.

8. $\Delta\theta = \dfrac{766 \times 10^3}{1.04 \times 10^9} = 7.36 \times 10^{-4}$ rads or 0.042 degrees.

APPENDIX II

Excerpt From

ADVANCED NUCLEAR SYSTEMS STUDY

Goddard Space Flight Center X-716-67-323

by

J. Epstein, D. W. Harris, and W. S. West

Dated July 1967

Pages 76 Through 88

ADVANCED NUCLEAR SYSTEMS STUDY (Excerpt)

D. MAGNETIC REQUIREMENTS

1. Acceptable Magnetic Flux Levels

The interplanetary magnetic field near the earth has a magnetic value of approximately five gamma, and a direction which is spiral and slightly below the Earth-Sun ecliptic plane. The magnetic field angle between the magnetic field and the Earth-Sun line is approximately 45° on Earth. This magnetic field description is an averaged measurement since there may be considerable magnetic field variation from measurement to measurement. Both the magnetic plasma flux and magnetic fields change markedly in periods of high solar activity.

The magnetic field is expected to decrease as the distance from the Sun to the spacecraft is increased, while the plasma flux is expected to decrease as the distance squared from the Sun to the spacecraft. Thus the plasma flux is expected to be decreased by a factor of 5^2 at five astronomical units, while the magnetic field should be down to approximately one gamma.

The major intent is to measure the magnetic fields down to approximately 0.5 gamma at 10 AU. Thus, a firm constraint can be made to ensure that the spacecraft magnetic field sum at the magnetometer location will be less than 0.1 gamma.

2. Expected Magnetic Flux

The expected magnetic flux, based on previous measurements of SNAP-9A and the IMP-RTG, is discussed on the following pages. These magnetic flux tests were performed on materials and components which could possibly be used in an RTG design. In addition to the magnetic flux tests, tests were performed on a SNAP-9A generator to determine the magnitude of the magnetic flux background.

a. SNAP-9A. Two tests were conducted with a SNAP-9A generator in the fueled and unfueled condition. The magnetic moment of the SNAP-9A generator was axial. The test results are given Figures 48 and 49.

No satisfactory explanation was found for the wide variance of test results in Figures 48 and 49. However, both tests demonstrate that neither the SNAP-9A materials nor the SNAP-9A design approach can be indiscriminately applied in the design of an RTG for the Galactic Jupiter Probe.

Distance and Condition	Short Circuited*		Open Circuit** (3 ft)
	(5 ft)	(3 ft)	
Type Magnetization	Radial Component (gamma)		
Permanent, initial	14.1	64	27
Induced, 14,500 gamma applied	—	5	—

*Generator output short circuited, i.e., maximum current
**Generator output open circuited, i.e., zero current

Figure 48. Radial Component of Magnetic Field, Fueled SNAP-9A Generator

Distance (ft)	5	3
Type Magnetization	Radial Component (gamma)	
Permanent, initial	79.5	358
Post 10 gauss exposure	--	369
Post deperming	--	317
Induced, 13,000 gamma applied	--	9

Figure 49. Radial Component of Magnetic Field, Unfueled SNAP-9A Generator

The SNAP-9A tests indicate the need for careful electrical circuit design and supporting tests to develop a satisfactory circuit with respect to stray fields.

b. SNAP-9A Fuel Capsule. Two tests were conducted on a fueled and an unfueled SNAP-9A fuel capsule. In both tests the magnetic moment was not detectable at a distance of 18 inches. The results of fuel capsule tests are given in Figure 50.

The fuel capsule tests demonstrate that insofar as magnetic characteristics are concerned, SNAP-9A type fuel capsules could be used in the Galactic Jupiter Probe-RTG design.

Condition	Fueled Capsule at Two Inches	Unfueled Capsule at One Inch
Type Magnetization	Radial Component (gamma)	
Permanent, initial	0.5	< 0.1
Post 25 gauss exposure	0.5	< 0.1
Post deperming	0.5	< 0.1
Induced, 13,000 gamma applied	< 0.2	< 0.1

Figure 50. Radial Component of Magnetic Field, SNAP-9A Fuel Capsule

c. Materials and Components Tests.

(1) Thermoelectric Element Components. A cast PbTe element and a hot and cold shoe of Type.821 stainless steel were tested as possible thermoelectric (T/E) element components. The results of the thermoelectric element + component tests are presented in Figure 51. The high values for the stainless steel cold shoe resulted from the cold rolling process used in element fabrication.

Type Magnetization	Radial Component at One Inch (gamma)		
	PbTe	Hot Shoe	Cold Shoe
Permanent, initial	Not detectable	1.0	16
Post 25 gauss exposure	Not detectable	1.0	20

Figure 51. Radial Component of Magnetic Field, Cast PbTe Thermoelectric Couple Components

(2) T/E Element Tests. Fifteen thermoelectric elements were tested. These were fabricated by hot pressing exclusively since cold pressed elements were not available at the time. Various shoe materials, bonding agents, and assemblies with iron diffusion barriers were tested. The results are presented in Figure 52.

As noted in Figure 52, those elements having Haynes-25 shoes, with tin as the bonding agent, gave the best results with respect to magnetic effects. The

Element No.	Date Tested	Element Type	Hot Shoe	Cold Shoe	Remarks	Radial Component of Magnetic Field Extrapolated to 18 In. (gamma)			
						Permanent, Initial	Post 25 Gauss Exposure	Post Deperming	Induced 20,000 Gamma
HP-4-3-1	5/22/63	N	0.050 in. 321 SS	0.050 in. 321 SS	Nickel bond	0.02	0.18	0.03	0
-4-3-2	5/22/63	N	0.050 in. 321 SS	0.050 in. 321 SS	Tin bond	0.01	0.08	0.02	0
-4-4-1	5/22/63	P	0.050 in. 321 SS	0.028 in. 321 SS	Tin bond	0.02	0.07	0.02	0
-4-4-2	5/22/63	N	0.050 in. 321 SS	0.050 in. 321 SS	Nickel bond	0.03	0.07	0.04	0
-4-5-1	5/22/63	N	0.0045 in. Haynes-25	0.0045 in. Haynes-25	Nickel bond	0.02	0.00	0.04	0
-4-5-2	5/22/63	P	0.0045 in. Haynes-25	0.0045 in. Haynes-25	Tin bond	Not perceptible at 18 in.			
-4-5-3	5/22/63	N	0.0045 in. Haynes-25	0.0045 in. Haynes-25	Tin bond	Not perceptible at 18 in.			
-5-8-1	6/3/63	P	0.050 in. 321 SS	0.010 in. 321 SS	Tin bond, 0.0017 in. Iron barrier	0.08	1.04	0.04	0
-5-8-2	6/3/63	P	0.050 in. 321 SS	0.010 in. 321 SS	Tin bond, 0.0017 in. Iron barrier	0.16	0.97	0.06	0
-5-9-1	6/3/63	P	0.050 in. 321 SS	0.010 in. 321 SS	Tin bond, 0.0017 in. Iron barrier	0.25	0.94	0.04	0
-5-9-2	6/3/63	P	0.050 in. 321 SS	0.010 in. 321 SS	Tin bond, 0.0017 in. Iron barrier	0.25	0.96	0.06	0
-5-9-3	6/3/63	P	0.050 in. 321 SS	0.010 in. 321 SS	Tin bond, 0.0017 in. Iron barrier	0.43	1.04	0.08	0
-5-9-4	6/3/63	P	0.050 in. 321 SS	0.010 in. 321 SS	Tin bond, 0.0017 in. Iron barrier	0.24	1.00	0.04	0
-5-9-5	6/3/63	P	0.050 in. 321 SS	0.010 in. 321 SS	Tin bond, 0.0008 in. Iron barrier	0.11	0.98	0.03	0
-5-9-6	6/3/63	P	0.050 in. 321 SS	0.010 in. 321 SS	Tin bond, 0.0008 in. Iron barrier	0.17	0.95	0.04	0

Figure 52. Thermoelectric Element Magnetic Tests

direction of the magnetic moments for the samples of Figure 52 are illustrated in Figure 53.

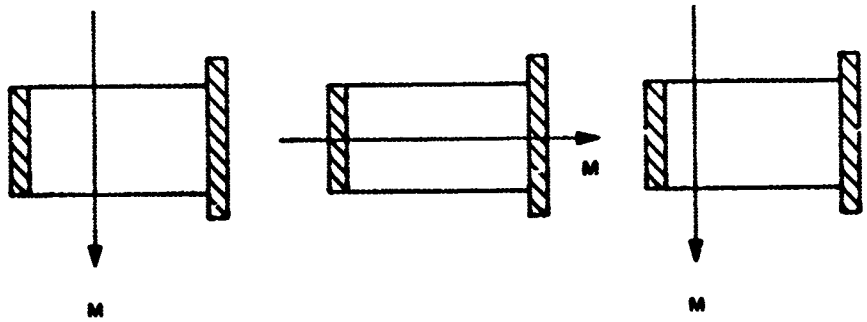

SAMPLE	SAMPLE	SAMPLE
HP-4-3-1	HP-4-3-2	HP-4-4-1
-4-5-1	-4-4-2	
-4-5-3	-4-5-2	
-5-8-1		
-5-8-2		
-5-9-1		
-5-9-2		
-5-9-3		
-5-9-3		

Figure 53. Magnetic Moments for Various Samples

d. Electrical Connector. Results of magnetic tests of an electrical connector used in the SNAP-9A design are given in Figure 54. A magnetic moment was not detectable when electrical connector was tested. Although the values in Figure 54 are not large, a connector having a lesser magnetic field will be required for the Galactic Jupiter Probe. This can be accomplished by proper design procedures.

Distance (in.)	18	36
Type Magnetization	Radial Component (gamma)	
Permanent, initial	<0.1	<0.013
Post 25 gauss exposure	0.3	<0.038
Post deperming	<0.1	<0.013
Induced, 26,000 gamma applied	0.3	<0.038

Figure 54. SNAP-9A Electrical Connector Magnetic Tests

e. Fuel Block. Type ATJ graphite was used as a fuel block for the SNAP-9A generator. Magnetic test results are presented in Figure 55. No significant magnetic moment was detected.

Distance (in.)	18	36
Type Magnetization	Radial Component (gamma)	
Permanent, initial	< 0.1	< 0.013
Post 25 gauss exposure	< 0.1	< 0.013
Post deperming	< 0.1	< 0.013
Induced, 26,000 gamma applied	< 0.1	< 0.013

Figure 55. Type ATJ Graphite Magnetic Tests

f. Other Items. Tests of other element components are summarized in Figure 56. These results are acceptable except for the iron cold sink springs. Inconel X was substituted for the spring material in the proposed design of the IMP-RTG. If the Galactic Jupiter Probe RTG utilizes a similar design, a suitable substitution such as Inconel X will also have to be made for this component.

	Radial Component at Two Inches (gamma)		
	Permanent, Initial	Post 25 Gauss Exposure	Induced, 26,000 Gamma Applied
Aluminum Cold Sink Bar (SNAP-11)	≤0.1	≤ 0.1	≤ 0.1
Aluminum Cold Sink Piston (SNAP-11)	≤0.1	≤ 0.1	≤ 0.1
Aluminum Cold Sink Button (SNAP-11)	≤0.1	≤ 0.1	≤ 0.1
Iron Cold Sink Spring (SNAP-11)	0.6*	0.6*	≤ 0.1*
Titanium Bolt, Washer, Nut	≤0.1	≤ 0.1	≤ 0.1

*At 13 inches

Figure 56. Radial Component of Magnetic Field-Other Items

g. Stray Fields. During the conceptual design effort for the IMP-RTG, it was determined that the electrical circuit within the generator would have to be designed to yield a minimum stray field effect. As noted by the results of the fueled SNAP-9A test (Figure 48), the initial permanent field was 64 gammas at short circuit and 27 at open circuit. This indicates the contribution of the circuit design. It was further determined that a satisfactory circuit design would require some experimental support. Accordingly, an electrical mockup of the generator was fabricated.

The mockup is shown in Figure 57. The simulated thermoelectric module bars were made of plexiglass. These were sized and oriented as were the actual module bars.

The simulated thermoelectric elements and associated electrical connections were made of copper wire. The thermoelectric circuit of each module was such that adjacent current paths were run in opposite directions. Tests were conducted at GSFC to determine a wiring pattern between modules and to develop compensating electrical loops.

The optimum basic module electrical circuit is shown in Figure 58. The current paths are shown schematically. This circuit resulted in a maximum stray field value of 115 gammas at 18 inches with a current flow of 5 amperes. A second series of tests were then performed to determine a compensating circuit.

A schematic of the recommended circuit, with compensation, is shown in Figure 59. Two compensating loops wired in parallel were used. The direction of current flow in each loop is the same. The reduction in field by the circuit is presented in Figure 60. During the tests, it was observed that exact placement of the two loops were required to obtain compensation. Thus, it will probably be necessary to compensate each RTG flight unit individually to reduce stray field effects.

3. Calculated Magnetic Flux From SNAP-27

The sources of magnetic field components for the SNAP-27 generator current flow, assuming that no material permeability effects exist, are shown in Figure 61. The contributing sources of magnetic field components are:

a. Ring Currents – Generator Ends. The ring currents will produce an axial component of magnetic field at the generator horizontal midplane. This contribution is potentially large and has been reduced by the addition of degaussing loops which have a current flow in a direction opposite to the ring currents at the ends of the generator.

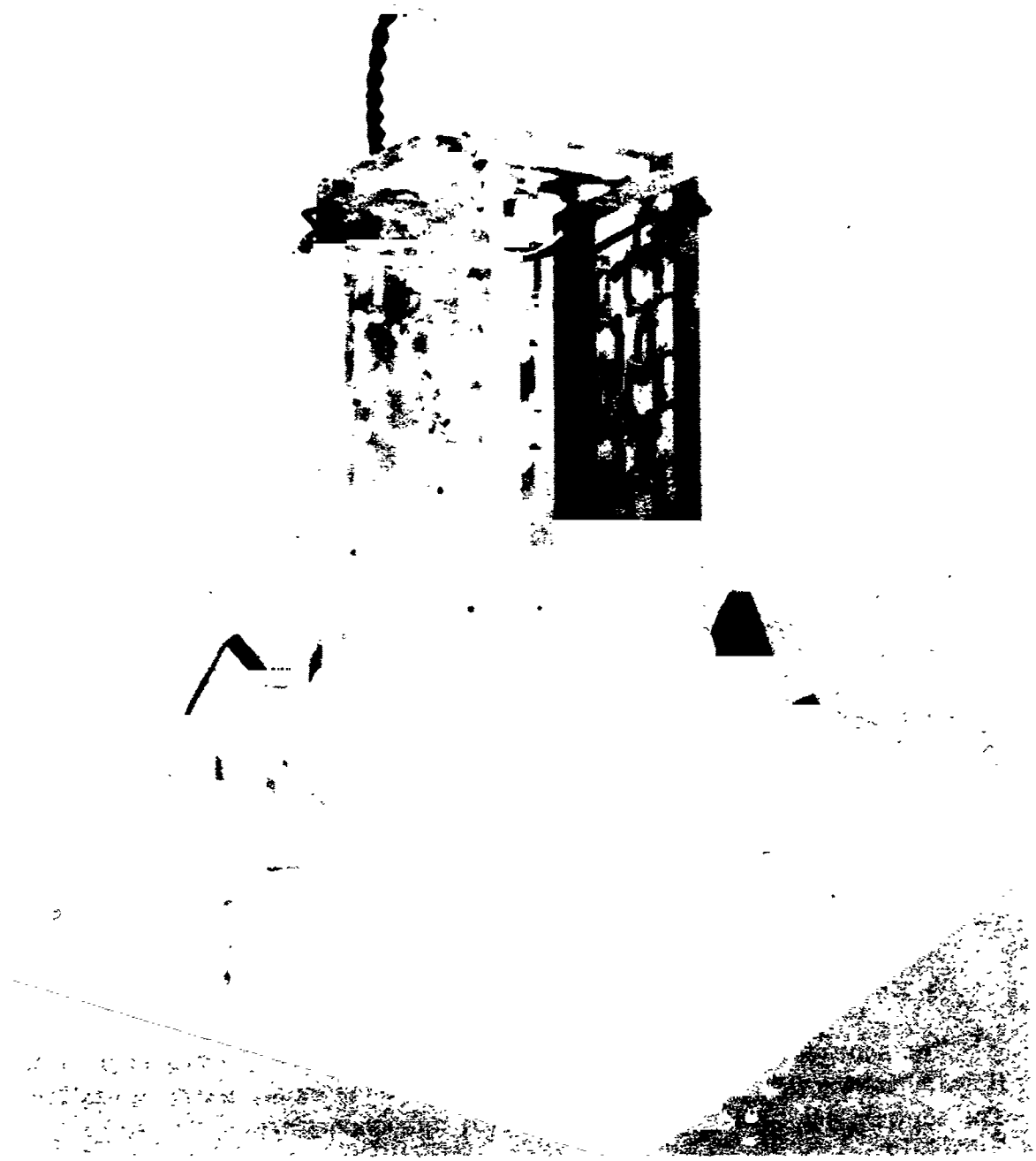

Figure 57. IMP RTG Electrical Mockup for Stray Magnetic Field Tests

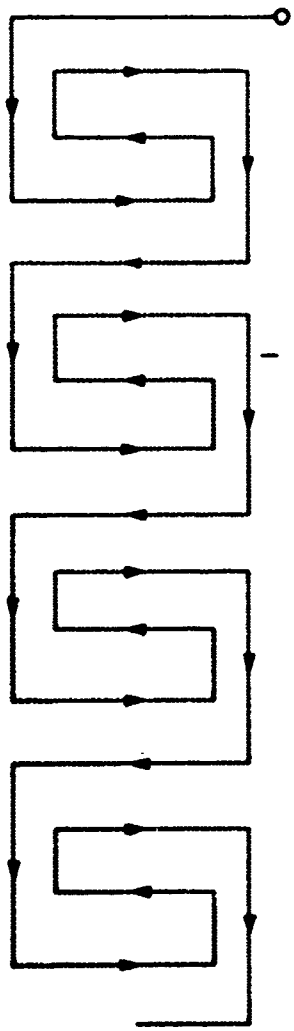

Figure 58. Circuit with Compensation Single Conductor

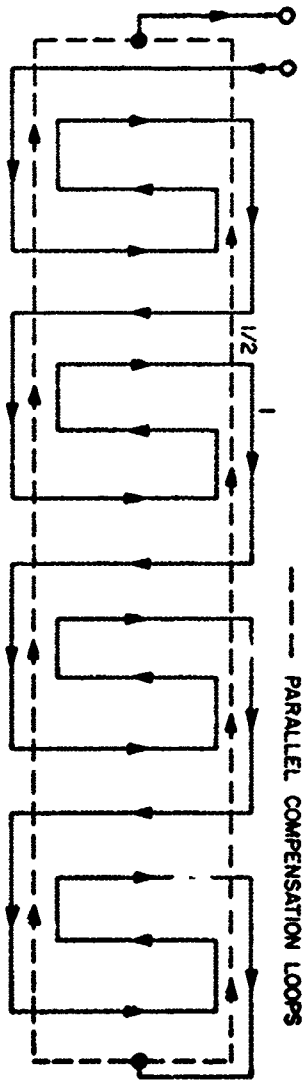

Figure 59. Circuit with Compensation, Parallel Loops

b. Longitudinal Current Flow. The longitudinal currents will produce a horizontal component of magnetic field. Since current flow direction in adjacent parallel rows is opposite, the resulting field would be expected to be small; however, a field assymmetry results because of the odd number of parallel rows (13). This asymmetry effect is reduced by conductors feeding the degaussing loops. Generator iron content is restricted to the electro-deposited iron on the hot shoes and the iron buttons on the thermocouple legs. The net effect of the depermed iron has been estimated to be a factor of 3 to 4 increase in magnetic field components over operation with non-magnetic material. The following information was used in assessing the total magnetic fields.

Orientation (degrees)		Circuit Compensation		
A	Z	ΔB_y	ΔB_z	ΔB_x
0	0	+8.5	+3.2	+2.3
90	0	-0.7	+2.4	+1.5
180	0	-0.6	+4.1	-1.8
270	0	+3.3	+3.9	-1.3
0	90	-6.8	-2.1	-0.9
0	270	-7.9	+2.6	-1.4
0*	20	+9.0	-0.7	+2.7
0*	250	-9.3	+0.6	-1.5

ΔB = difference between current off and current on conditions.
*Peak
Measurements at 18 inches

Figure 60. IMP-RTG Stray Field Magnetic Compensation

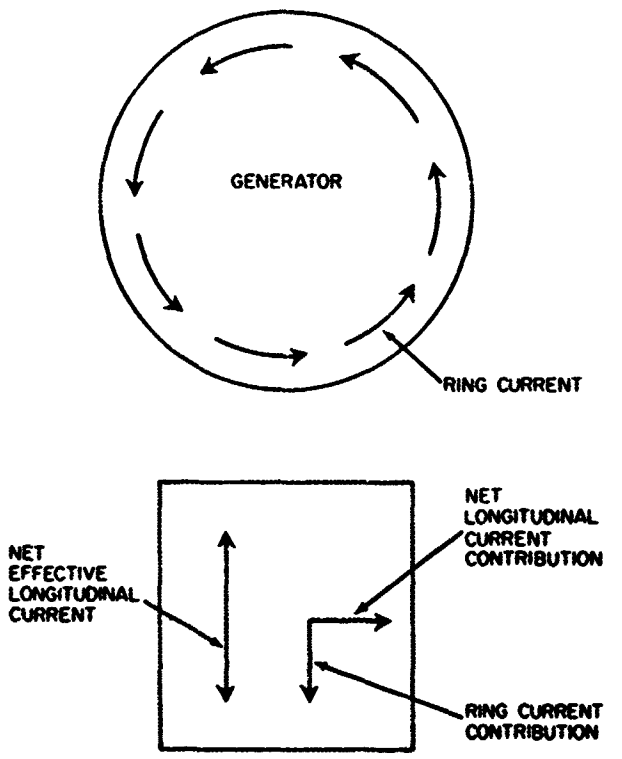

Figure 61. SNAP-27 Generator Magnetic Field Components

c. Ring Current/Degaussing Loop. The field due to the ring currents, in gammas/ampere, is shown in Figure 62. The values shown reflect the estimated iron-content contribution and degaussing loop operation.

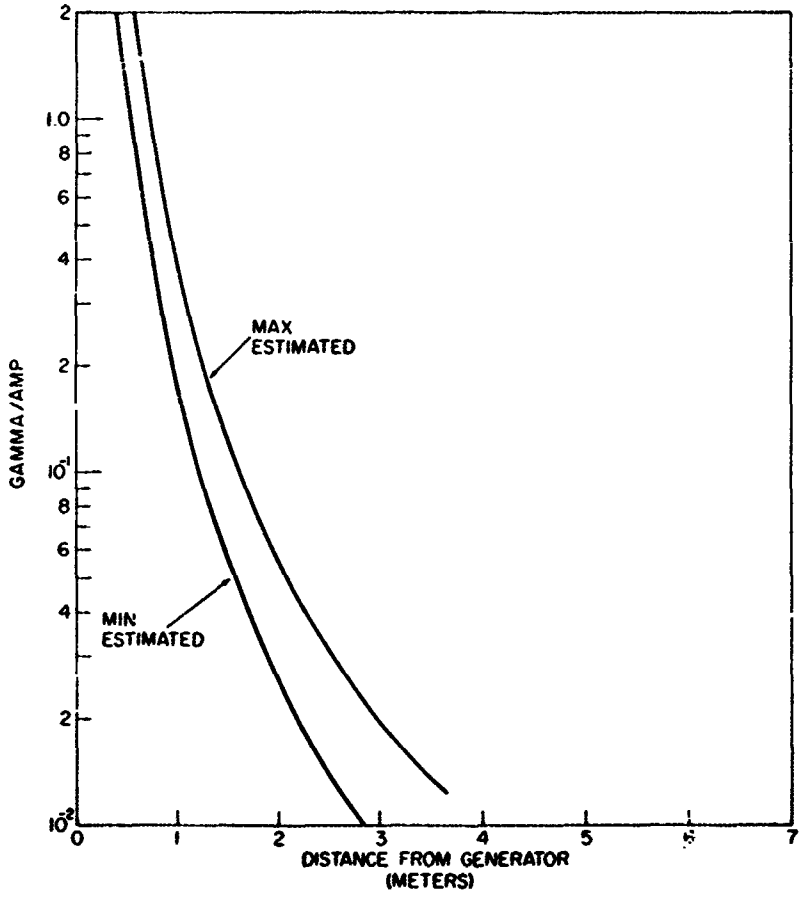

Figure 62. SNAP-27 Generator Axial Magnetic Fields

d. Longitudinal Currents. The field due to longitudinal currents is shown in Figure 63. A factor of 3 to 4 for iron content has been included in this curve.

When all effects are taken into account, the results indicate that the total magnetic field at a distance of 3 meters from the RTG should be less than 0.05 gamma. At 10 meters, the total magnetic field from 2 RTGs will be significantly less than 0.1 gamma.

4. Measured Magnetic Fields From SNAP-27

Magnetic field measurements of the SNAP-27, Model 8B engineering generator assembly were performed at the GSFC-Component Magnetic Test Facility on

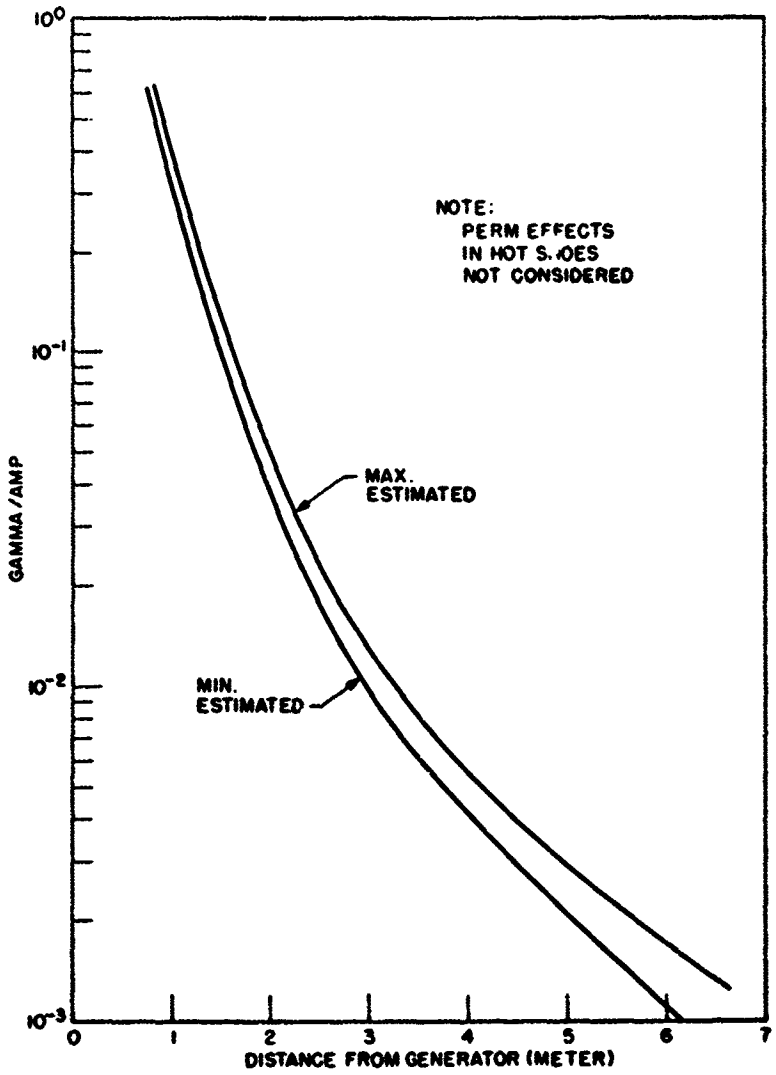

Figure 63. SNAP-27 Generator Longitudinal Magnetic Fields

27 and 28 April, 1967. The objective of the tests was to determine the permanent, induced, and stray magnetic field disturbance of the RTG assembly. Figure 64 presents the results of these measurements.

During the tests the assembly was referenced so that the X-axis was always the primary axis with the set of fins aligned with the output cable (-Y side) representing the Y-axis. Throughout the permanent and induced field measurements, the peak values occurred in the X-axis direction of the assembly with a lesser opposite peak lying in an off axis (+X, -Y) direction. This non-symmetrical field can be attributed to the fact that the magnetic dipole moment does not fall in the geometrical center of the RTG assembly. The significant field reduction

Test Condition	Distance			
	2 Feet	3 Feet	4 Feet	6 Feet
Perm plus Induced (0.13G)	80.3*	18.2*	6.8*	2.1*
Initial Perm	81.8	20.0	7.6	2.1
Post 15G Exposure (X-axis)	233.0	59.4	23.5	6.4
(Y-axis)			4.2	
Post 50G Deperm	1.1	0.2	0.2	0.2
Induced (0.26G)	14.6	4.2	1.6	0.5
Induced (0.26G) (Assembly Depermed)	15.1	4.0	1.6	0.5
Stray Fields				
1 AMP	4.8	2.2	1.1	0.3
3 AMPS	21.7	6.8	2.6	0.8
4 AMPS	30.0	8.5	3.7	1.2
6 AMPS	43.7	12.7	5.4	1.7
8 AMPS	58.4	17.2	7.4	2.2

*All values in gamma (10^{-5} gauss)

Figure 64. SNAP-27, Model 8B Magnetic Fields

achieved by the deperm treatment is evidence of the value of performing the magnetic survey and deperm following the other phases of environmental testing (especially vibration). However, further measurements are recommended in order to establish the final remanent perm level the unit obtains after deperming and ambient field exposures.

The stray field data presents the fields generated by the various current levels. Since the magnitudes measured along the y and z faces were nearly equal, a resultant off-axis peak was obtained (y-z plane).

The Model 8B assembly contained ten iron-constantan thermocouples that will not be present in the flight units. These thermocouples have affected the results but the magnitude of this effect is not known at the present time.

Examination and interpolation of the data indicates that the field at 6 feet from the RTG will be 7.5 gamma (6.4 gamma after post 15 gauss exposure +1.1 gamma stray fields). If this value is extrapolated to 21 feet (separation distance for RTG and magneto-meter assuming a 15 foot experiment boom) the resultant field from one RTG is 0.175 gamma or 0.35 gamma for both RTGs assuming their fields sum at the magnetometer. Although this value exceeds the desired level of 0.1 gamma at the magnetometer, the proper use of degaussing loops to reduce stray fields and further experimental results to verify the final remanent perm field will undoubtedly help to reduce the magnetic field to an acceptable level. Further reduction in the fields can also be achieved if the iron discs used in the generator assembly are replaced by a nonmagnetic material.

5. Magnetic Fields From SiGe Thermoelectric Material

A segment of a SNAP-17 module was tested at the GSFC Magnetic Test Facility. This material, in the configuration of the SNAP-17 module, exhibited no magnetic moments, and no significant fields were detected.

6. Methods to Reduce Magnetic Flux Levels.

There are several options available to the designer for reducing magnetic flux levels. The use of non-magnetic materials is an obvious choice. However, if a PbTe thermoelectric generator is utilized, it may be necessary to use iron components in module fabrication. A possible substitution for the iron shoes is tungsten. Development of tungsten shoes for PbTe couples is presently being carried out and this process may be available for a 1972 launch.

Another method frequently used to reduce flux levels is to locate the magnetic source and the magnetometer as far apart as possible. This technique works satisfactorily if the magnetic fields are small and the background requirements for the magnetometer are greater than 0.5 gamma. All RTGs produce stray magnetic field because they are inherently high electric current sources. These stray fields may be reduced by designing the thermoelectric modules in a symmetric array and incorporating wiring loops constructed such that the current flow tends to reduce stray field generation. Compensation loops may also be incorporated to further reduce these fields.

APPENDIX III

Memorandum

by

A. W. Fihelly

re

SNAP-19 S/N 009 MAGNETIC MOMENTS MEASUREMENT

UNITED STATES GOVERNMENT MEMORANDUM

To: Harry Press
Nimbus Project Manager

Date: 23 December 1968

From: A. W. Fihelly
Nimbus Project Office

Subject: SNAP-19 S/N 009 Magnetic Moments Measurements; comments concerning

Enclosure: (1) Preliminary Test Report of 10 December, same subject
(2) Preliminary Test Report of 3 April for S/N 008A, same subject

In the period 9 - 11 December 1968, the SNAP-19 flight RTG for Nimbus B2 was at the Goddard Magnetic Test Facility for magnetic moments measurements and final deperming prior to delivery to General Electric. The test set-up was as follows: standoff S/N 005 was bolted to a wooden box, with PCU S/N 003 inside, and the generators and tripod bolted to the standoff. The wooden box was bolted to the MFT moveable dolly, shimmed with a 5- inch wooden disc to get RTG center of magnetic mass within an inch of coil center. Magnetic moments were measured as received (generators shorted and I_{max} flowing), and on dummy load (the generators on PCU which was on a remote load - less current flowing). The system was sequentially permed in the X-, Y-, Z- field axes by a 15 Gauss field, then depermed in a 50 Gauss AC field. Finally, the magnetic moments induced by a 0.3 Gauss X-, Y-, Z- field, approximately the Earth's field for a 50 nm orbit, were measured. Enclosure (1) summarizes the test data for SNAP-19 S/N 009.

It is of interest to compare S/N 009 data with similar data taken for the last flight SNAP-19 system, S/N 008A, tested at GSFC in April 1968. These data are presented in Enclosure (2). It is apparent that S/N 008A had a much higher as received moment than S/N 009, 4600 pole-cm to 1589, or a factor of 2.89 higher. In X-perm, S/N 008A was higher 4700 pole-cm to 3010, but could be depermed to a lower value 735 pole-cm to 854. In Y-perm, S/N 009 was higher 2209 pole-cm to 1540, but could be depermed to a lower value 725 pole-cm to 800. In Z-perm, S/N 009 was higher 1834 pole-cm to 1600, but could be depermed to a lower value 659 pole-cm to 870. One interesting feature of the S/N 008A and S/N 009 data is that the residual moment after deperms one through three increased from 735 to 870 pole-cm for S/N 008A, but decreased

from 854 to 639 pole-cm for S/N 009. In both cases, the final depermed moments are less than 900 pole-cm, which should pose no problem for the Nimbus B2 controls.

The induced moments from a 0.3 Gauss X-, Y-, Z- axis field are seen to be little different than the post third deperm value.

Data were also taken with the generators open circuited (no current flow) briefly as the power connector was changed from dummy load to short circuit to get the effect of various current loops. The effects of test rig, PCU, standoff, and test harness were measured ipso facto and found to be insignificant. The only key component not measured by itself was the heavy stainless steel tripod and isolation mount, long the suspected culprit in the high "as received" values and the system element nearest the MBC-210 shaker's mounting plate and 40 - Gauss field during the final Z-axis flight level shake at Martin. In an effort to pin this down, C. F. Baxter will have a SNAP-19 tripod vibrated in the near future in flight configuration and brought to GSFC for magnetic measurement.

A. W. Fihelly
Nimbus Project Office

cc: W. B. Huston
S. Weiland
G. Burdett
H. Damare
H. Nichols
C. Thienel
P. Crossfield
G. Delio
Dr. W. Redisch
C. F. Baxter, AEC/GSFC
W. S. West
J. Epstein
V. Redmond (Sandia)

(PRELIMINARY) REPORT OF AN ENVIRONMENTAL TEST

GENERAL INFORMATION

1. PROJECT	2. TYPE TEST	3. TAR. NO.	4. TEST DATE
NIMBUS – B	Magnetic		3 April 68

5. TEST ITEM	6. MODEL	7. SERIAL NUMBER
SNAP-19 Type 08A	08A	

8. ITEM LOCATION IN S/C: (IF S/C TEST, AXES ORIENTATION)	9. TEST EQUIPMENT/FACILITY
X-axis Roll; Y-axis Pitch; Z-axis Yaw	ACTF

10. TEST OBJECTIVES

Determine magnetic moment along each axis. Deperm if required.

TEST PERSONNEL

11. TEST COORDINATOR	12. EVALUATION ENGINEER
Woodward	W. D. Kenney – C. L. Parsons
13. PROJECT MANAGER REPRESENTATIVE	**14. DESIGN GROUP REPRESENTATIVE/EXPERIMENTER**
Fihelly	G. E.

TEST SET-UP

15. INSTRUMENTATION:

Forster Magnetometer Mod. 5050 (3)	
Brush 8-channel Recorder (2)	
MADAS Digital data acquisition system	
ACTF 40 ft coil	
Deperm coils, 5 ft & 10 ft	

16. TEST SPECIFICATIONS:

17. TEST PROCEDURE

SNAP-19 Fueled RTG Power Supply – Magnetic Moment Test (2nd Edition)
Dated 1 April 68

18. PREPARED BY:	19. COORDINATION:
C. L. Parsons — EVALUATION ENGINEER	W. H. Woodward — TEST COORDINATOR

DISTRIBUTION: SCHEDULE "( )"

320-4 (10/68) GODDARD

PROJECT NIMBUS
ITEM SNAP-19 (08A)
TEST DATE 3 April 68

(PRELIMINARY) REPORT OF AN ENVIRONMENTAL TEST

(CONTINUATION SHEET)

(CONTINUATION OF ANY SECTION WHERE MORE SPACE IS REQUIRED

MAGNETIC MOMENT (in C.G.S. pole-centimeters)

	Mx	My	Mxy	Mz	Mt
Initial (Shorted)	2800	24	2800	3660	4600
(Dummy)	2620	171	2620	3420	3890
Post 15 G. X-axis	3720	215	3720	3420	4700
Post 1st Deperm	730	100	730	245	735
Post 15 G. Y-axis	630	1400	1535	245	1540
Post 2nd Deperm	755	159	795	245	800
Post 15 G. Z-axis	860	86	915	1320	1600
Post 3rd Deperm	790	120	835	245	870

Roll	Pitch	Yaw
758	126	245

Since this SNAP-19 was placed on a vibration machine of the MB C-210 type on two occasions, there is every reason to believe that the high magnetization found originated from that source. Measurement of the vertical field on a C-210 indicated magnitudes of 40 gauss on the surface plate, 25 gauss at 1 inch above, 15 gauss at 4 inches above, 8 gauss at 8 inches above, etc. Deperm treatment removed 80 percent of the total magnetic moment (93 percent of the vertical moment). There was no sigrificant increase in this moment after 17 hours in the shorted mode, nor after 2 hours in the dummy load mode.

The maximum moment expected in the Y-axis (pitch) is 1400 pole-centimeters and this would occur only if a 15 gauss exposure should take place. The present value is 120 pole-centimeters and it is highly improbable that this value would rise to more than 500 pole-centimeters due to shock and vibration in earth ambient field.

C. Leland Parsons (Code 325)
Magnetic Test Section

320-4c (10-63) GODDARD

PAGE ___ OF ___

(PRELIMINARY) REPORT OF AN ENVIRONMENTAL TEST

GENERAL INFORMATION

1. PROJECT	2. TYPE TEST	3. TAR. NO.	4. TEST DATE
NIMBUS – B	Magnetic	16399	Dec. 10, 1968

5. TEST ITEM	6. MODEL	7. SERIAL NUMBER
SNAP 19		S/N 9

8. ITEM LOCATION IN S/C: (IF S/C TEST, AXES ORIENTATION)	9. TEST EQUIPMENT/FACILITY
X-axis Roll; Y-axis Pitch; Z-axis Yaw	ACTF

10. TEST OBJECTIVES

Determine magnetic characteristics as per test procedure

TEST PERSONNEL

11. TEST COORDINATOR	12. EVALUATION ENGINEER
W. H. Woodward	C. L. Parsons
13. PROJECT MANAGER REPRESENTATIVE	**14. DESIGN GROUP REPRESENTATIVE/EXPERIMENTER**
A. W. Fihelly	C. Baxter; S. Macarevich

TEST SET-UP

15. INSTRUMENTATION:

Forster Magnetometer Mod. 5050 (4)	
Brush 8-channel Recorder (2)	
MADAS Digital data acquisition sys.	
ACTF 40 ft coil	
Deperm coils, 5 ft & 10 ft	

16. TEST SPECIFICATIONS:

17. TEST PROCEDURE:

SNAP – 19 Fueled RTG Power Supply – Magnetic Moment Test (2nd Edition dated 1 April 68)

18. PREPARED BY:	19. COORDINATION:
C. L. Parsons – J. Boyle EVALUATION ENGINEER	W. H. Woodward TEST COORDINATOR

DISTRIBUTION: SCHEDULE "( )"

PROJECT NIMBUS-B
ITEM SNAP – 19 S/N9
TEST DATE Dec. 10, 1968

(PRELIMINARY) REPORT OF AN ENVIRONMENTAL TEST

(CONTINUATION SHEET)

(CONTINUATION OF ANY SECTION WHERE MORE SPACE IS REQUIRED.)

MAGNETIC MOMENT (in C.G.S. pole-centimeters)

	Mx	My	Mxy	Mz	Mt
Initial (Shorted)	1087	178	1101	1146	1589
(Dummy)	994	288	1034	1187	1574
Post 15 G. x-axis	2688	416	2720	1290	3010
Post 1st Deperm	532	406	669	530	854
Post 15 G. Y-axis	600	2062	2148	516	2209
Post 2nd Deperm	408	399	571	446	725
Post 15 G. Z-axis	573	406	702	1694	1834
Post 3rd Deperm	350	429	554	356	659
Post Induced (Dummy)	380	384	540	356	647
(Shorted)	442	355	567	266	626
Induced 0.3 G. +X	459	38		290 ± 90	
Induced 0.3 G. +Y	-25	509		-122 ± 122	
Induced 0.3 G. +Z	330	-98		328	

The induced moments reported above are the values obtained by subtracting the moments in zero field from the moments observed with 0.3 Gauss applied. The X and Y components of induced moment were essentially independent of azimuth. The Z component, however, varied with azimuth when the inducing field was applied in the +X or +Y directions. This variation is denoted by a plus or minus quantity applied to the average value of the induced moment.

APPENDIX IV

SNAP-19 MAGNETICS MOMENTS MEASUREMENTS — APRIL 1969

by

D. W. Harris

SNAP-19 MAGNETICS MOMENTS MEASUREMENTS — APRIL 1969

In April 1969 as this report is being prepared for publication, Goddard is performing magnetic moments tests on a SNAP-19 system, number 2A.

In these tests, the SNAP-19 system is being tested as a complete system less fuel. Further, the system has been separated into its major elements and tested further. The data have not been analyzed and no specific conclusion is available. In preliminary discussions with test personnel, it appears that data from these tests are consistent generally with the previously reported test conducted at Goddard on field SNAP-19 systems. In general, the magnetic fields associated with this system may be considered to arise primarily from each of the following elements:

— the two generators

— the power conversion unit

— the mount

— the Cabling-Harness.

Each contributed a measurable and significant amount.

APPENDIX V

Letter From

N. F. Campbell
Isotopes Nuclear Systems Division
of Teledyne Company

to

W. S. West
Goddard Space Flight Center

re

SNAP 19 MAGNETIC FLUX DISTRIBUTION

PRECEDING PAGE BLANK NOT FILMED.

ISOTOPES
NUCLEAR SYSTEMS DIVISION
EASTERN BLVD AT MARTIN BLVD N E
P O BOX 4937
MIDDLE RIVER, MARYLAND 21220
(301) 682-5800 TWX (710) 239-9037

A TELEDYNE COMPANY

Refer to: 00999-05-29-69

May 29, 1969

Mr. William West, Code 701
National Aeronautics and Space Administration
Goddard Space Flight Center
Greenbelt, Maryland 20771

Dear Mr. West:

In response to your telephone request of last week, I am enclosing a write-up entitled "SNAP 19 Magnetic Flux Distributions." This is the information you desired for incorporation into your Goddard report dealing with magnetic considerations as they pertain to spacecraft applications.

If you have any questions, please give me a call.

Sincerely,

R Rivelaun, for

N. F. Campbell
Program Manager
SNAP 19 Program

Enclosure

cc: B. Rock, AEC/HQ (w/encl)

APPENDIX V

SNAP 19 MAGNETIC FLUX DISTRIBUTION

A matter of interest to the spacecraft designer is the magnetic flux distribution surrounding the SNAP 19 subsystems. In this section it is shown, using an approximate model, that the flux from each subsystem (pair of generators), owing to the means of pairing the generators, decreases like $1/Z^4$. The approximate results show a flux from a single subsystem which is about a decade smaller than the Pioneer flux criterion of 0.05 gamma at the magnetometer (10 meters from the center of the subsystem).

ANALYSIS

The physical model for the current circuits in the SNAP 19 is shown in Figure 1. At the left is shown the intermodule wiring for a single generator. The right hand portion of this illustration shows the current loop model for the subsystem. This current loop is further reduced to 4 circular current loops (peripheries of shaded regions of Figure 1) where the current has positive sense in the upper loops and negative sense in the lower loops. The vertical portions of the loops give rise to field components which cancel in pairs along the Z-axis. (Experimental evidence indicates that the axial flux exceeds that in the midplane at the same separation distance by a factor of five. All calculations presented here are done, therefore, at axial detector points.) Thus the model comprises 2 pairs of oppositely directed current loops symmetrically placed with respect to the center of the subsystem.

The general behavior of the axially directed magnetic intensity vector at points along the axis may now be determined in terms of this model. Consider the resultant field from either pair of current loops, the loops being located at $\pm Z_o$ relative to the center. At any axial detector point (O, O, Z) the near loop contributes a positive flux while the far loop contributes a negative flux, smaller in magnitude. The equations shown in Figure 2 give the binominal expansion for the positive term B_1 and the negative term B_2 in terms of the quantities Z_o/Z and R/Z, where R is the loop radius. At remote detector locations ($Z > 3$ meters) these quantities are both small compared to unity so that second order terms in the quantity B_1-B_2 may be ignored.

The total flux is thus shown to vary in first order as Z^{-4}. It depends linearly on Z_o, as it should, since we expect the flux to vanish identically as Z_o approaches zero. The result for the 4 current loops comprising the model for a subsystem,

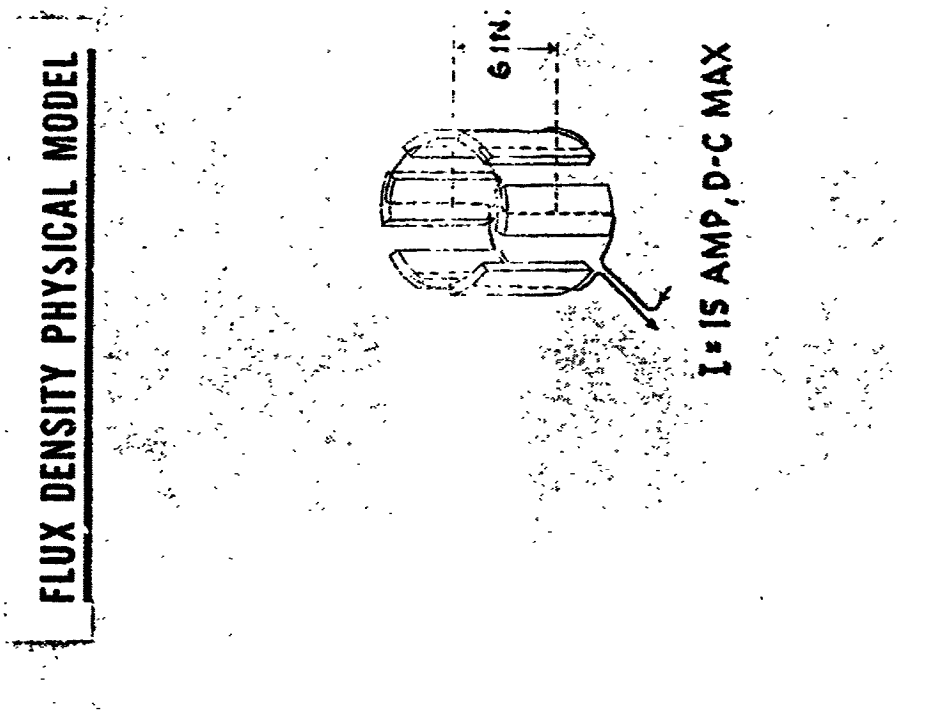

Figure V-1

MAGNETIC FLUX FROM LOOP PAIR

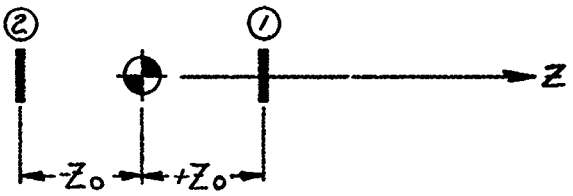

$$\frac{B_1}{C} = \frac{1}{[R^2+(Z-Z_0)^2]^{3/2}} = \frac{1}{Z^3}\,\frac{1}{\left[\left(\frac{R}{Z}\right)^2+\left(1-\frac{Z_0}{Z}\right)^2\right]^{3/2}}$$

$$= \frac{1}{Z^3\left[1-\frac{2Z_0}{Z}+\left(\frac{Z_0}{Z}\right)^2+\left(\frac{R}{Z}\right)^2\right]^{3/2}} = \frac{1}{Z^3(1-X)^{3/2}}$$

WHERE $X = 2\frac{Z_0}{Z} - \left(\frac{Z_0}{Z}\right)^2 + \left(\frac{R}{Z}\right)^2$

$$\frac{B_1}{C} = \frac{1}{Z^3}\left(1+\frac{3}{2}X+\frac{15}{8}X^2+\frac{105}{48}X^3+\ldots..\right)$$ BINOMIAL SERIES EXPANSION

$$\frac{B_2}{C} = \frac{1}{[R^2+(Z+Z_0)^2]^{3/2}} = \frac{1}{Z^3\left[1+\frac{2Z_0}{Z}+\left(\frac{Z_0}{Z}\right)^2+\left(\frac{R}{Z}\right)^2\right]^{3/2}} = \frac{1}{Z^3(1+Y)^{3/2}}$$

WHERE $Y = 2\frac{Z_0}{Z} + \left(\frac{Z_0}{Z}\right)^2 + \left(\frac{R}{Z}\right)^2$

$$\frac{B_2}{C} = \frac{1}{Z^3}\left(1-\frac{3}{2}Y+\frac{15}{8}Y^2-\frac{105}{48}Y^3+\ldots..\right)$$

$$\frac{B_1-B_2}{C} = \frac{1}{Z^3}\left(\frac{3}{2}[X+Y]+\frac{15}{8}\underbrace{[X^2-Y^2]}_{0}+\frac{105}{48}\underbrace{[X^3+Y^3]}_{0}\ldots..\right)$$

$$X+Y \cong \frac{4Z_0}{Z}$$

$$B_{TOTAL} = B_1-B_2 = \frac{C6Z_0}{Z^4} \qquad \boxed{B_{TOTAL} \sim \frac{1}{Z^4}}$$

Figure V-2

therefore, consists of two terms each positive and varying like Z^{-4}, so that the total flux from a subsystem varies as Z^{-4} at distances greater than about 3 meters.

Figure 3 shows this result graphically for a single pair of current loops. The curves marked B_1 and B_2 representing the absolute value of the magnetic flux, each vary nearly as Z^{-3}. Their difference, labeled B total, varies as Z^{-4} at large separation distances.

Figure 4 presents calculations performed using this approximate model for a SNAP 19 subsystem. For the purposes of this calculation, a maximum current of 15 amperes was assumed in the loops. It is seen that a minimum separation distance (from the magnetometer) of about 6 meters would be required for 2 subsystems so as not to exceed the criterion of 0.05 gamma at the magnetometer. At a separation distance of 10 meters the flux from a single subsystem is about 1/10 of the limiting value.

(Note that the test point shown in Figure 4 is inappropriate. It was determined for a single generator rather than a pair. The calculated flux at this distance from the center of a single generator, however, agreed well with the measurement, thus substantiating to some extent, the validity of representing the generator by two current loops.)

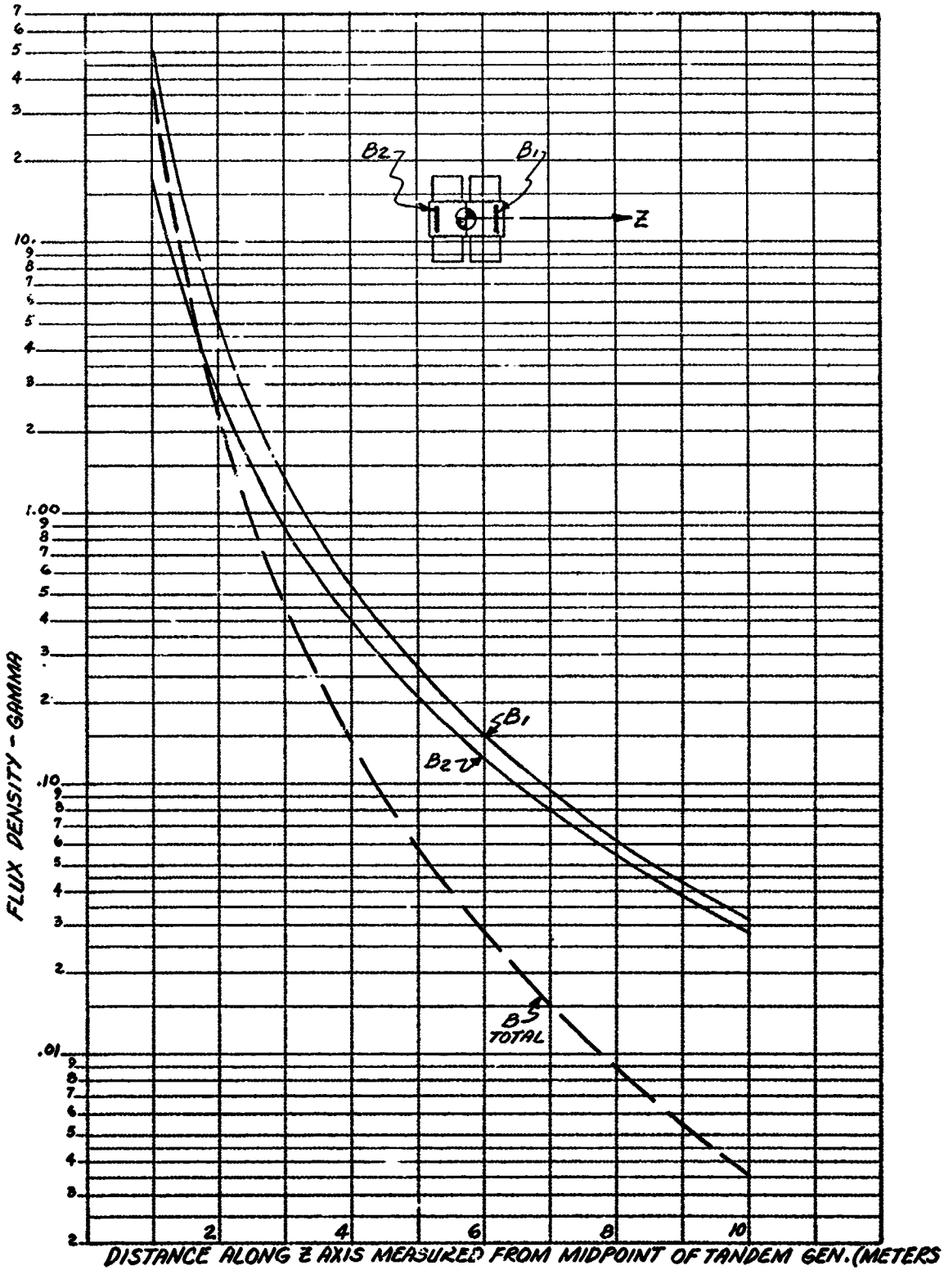
FLUX DENSITY - GAMMA
DISTANCE ALONG Z AXIS MEASURED FROM MIDPOINT OF TANDEM GEN. (METERS
B2
B1
Z
B1
B2
B
TOTAL

Figure V-3

SNAP 19 MAGNETIC FLUX DENSITY FIELDS

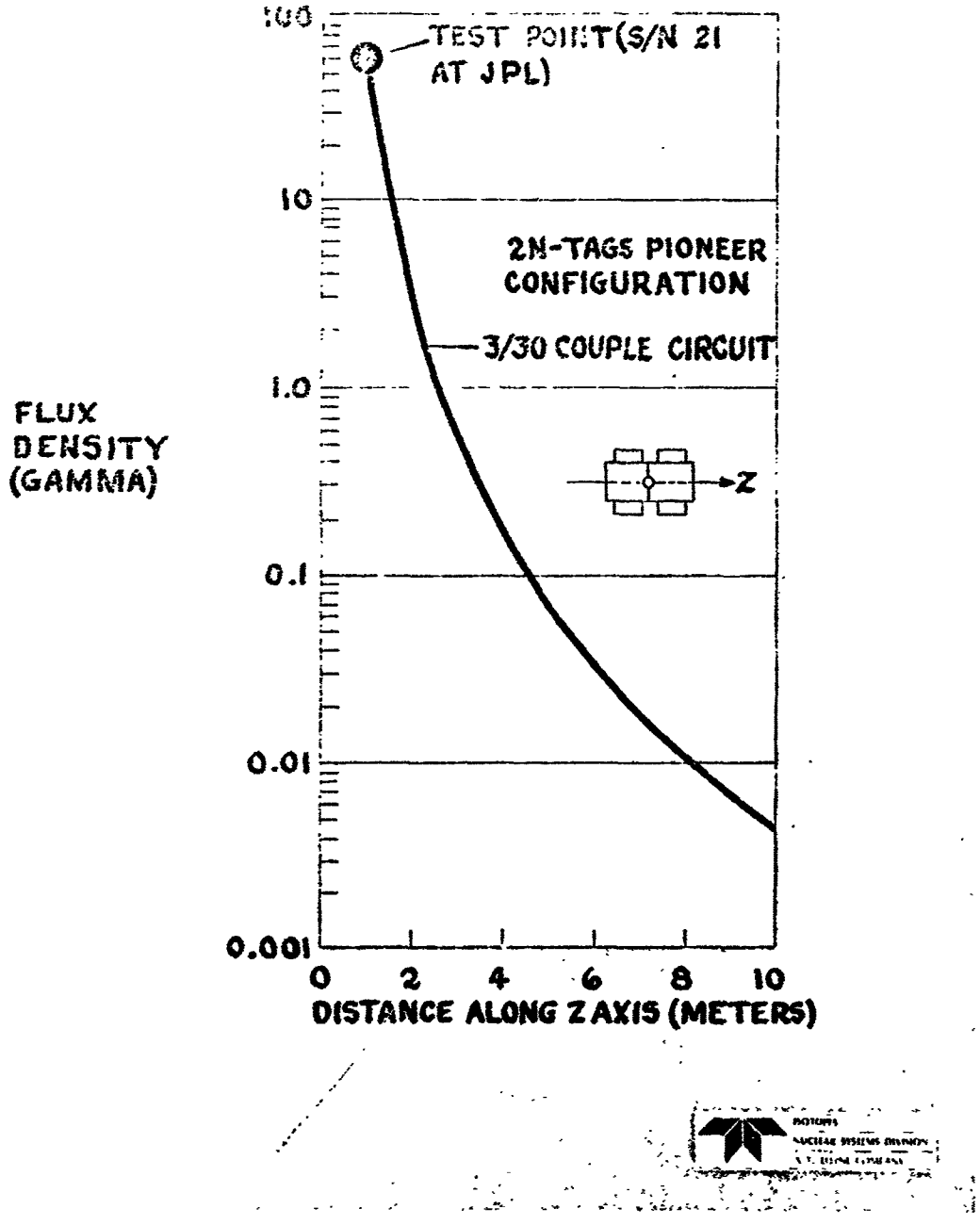

Figure V-4